Journal of Molecular Modeling (2026) 32:202
https://doi.org/10.1007/s00894-026-06774-9

RESEARCH

Singlet fission tinkertoys based on N-heterocyclic carbenes: the role of stereoisomerism

Joanna Stoycheva[1] · Rumen Lyapchev[1] · Alia Tadjer[1] · Marc de Wergifosse[2] · Julia Romanova[1,3]

Received: 19 November 2025 / Accepted: 8 May 2026 / Published online: 25 May 2026

Abstract

Context This theoretical study reports excited states molecular design of potential singlet fission materials based on homo- and heterodimers of N-heterocyclic carbenes (NHCs) and their "locked" analogues. We found that the electronic properties of the investigated compounds can be finely adjusted by an interplay of the following factors: diradical character, topology, type of substituents, extension of the π-conjugation, excited state aromaticity, length of the latch in the "locked" analogues, conformation, and even stereoisomerism. With focus on the stereochemical aspects, this work provides new insights into the molecular design principles for diradicaloid organic materials with attractive electronic and excited state properties. Based on the comprehensive analysis, seventeen compounds were identified as promising candidates for efficient singlet fission.

Methods Due to the large molecular size of the compounds and the importance of both static and dynamic correlation effects, the theoretical study is executed using simplified quantum chemistry (sQC) methods as screening tools, demonstrating their good performance in singlet fission aspect. Excited-state properties and singlet fission propensity of the NHC dimers were evaluated implementing spin-flip simplified time-dependent density functional theory (SF-sTD-DFT) and unrestricted simplified TDA (UsTDA) calculations. Vertical excitation energies and diradical characters were determined to assess the energetic conditions for singlet fission and to rationalize the effect of topology, substitution, and stereochemistry.

Keywords Diradical character · Spin-flip · SF-sTD-DFT · Electron rich olefins · Tetraazafulvalenes · Photovoltaics

Introduction

Lately, the interest in organic photovoltaics has been renewed because of the renaissance of singlet fission — a photophysical process, which can boost solar cell efficiency beyond the Shockley–Queisser limit [1]. In singlet fission, the energy of one absorbed photon is converted into two triplet excitons. Therefore, if utilized in solar cells, singlet fission may improve their performance by doubling the number of generated charge carriers per absorbed photon [2]. The implementation of singlet fission augurs a bright future for organic photovoltaics. Before this potential could be fully realized, however, we have to unearth the structure-properties relationship enigmas of the molecules able to undergo this process.

Indeed, singlet fission chromophores should satisfy a long list of requirements [3, 4]. First of all, twice the excitation energy from the singlet ground state to the first triplet excited state should be equal to or less than the excitation energy to the first singlet excited state, $\Delta E_{ST} = 2E(T_1) - E(S_1) \lesssim 0$. Second, twice the excitation energy to the first triplet excited state must be less than the excitation energy to the second triplet excited state, $\Delta E_{TT} = 2E(T_1) - E(T_2) < 0$. From a thermodynamic point of view, these two requirements are the primary singlet fission prerequisites, known as *feasibility conditions* (Scheme 1). They ensure that singlet

The preprint of the paper is uploaded to the ChemRxiv website under 10.26434/chemrxiv-2022–56571.

✉ Marc de Wergifosse
marc.dewergifosse@uclouvain.be

✉ Julia Romanova
jromanova@chem.uni-sofia.bg

[1] Faculty of Chemistry and Pharmacy, Sofia University "St. Kliment Ohridski", 1 James Bourchier Blvd., Sofia 1164, Bulgaria

[2] Theoretical Chemistry Group, MOST Division, Institute of Condensed Matter and Nanosciences, Université Catholique de Louvain, Place Louis Pasteur 1, B-1348 Louvain-La-Neuve, Belgium

[3] Research and Development and Innovation Consortium, 111 Tsarigradsko Shosse Blvd., 1784 Sofia, Bulgaria

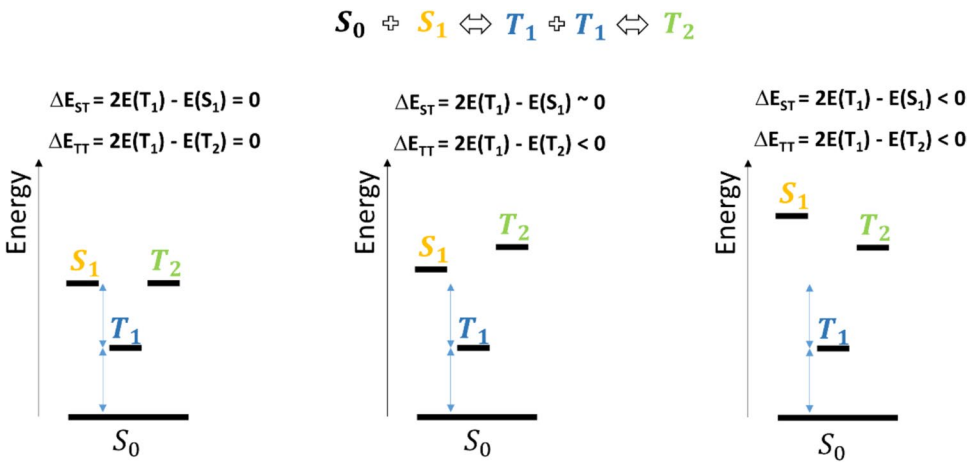

Scheme 1 Possible excited states alignments in chromophores, which satisfy both feasibility conditions for singlet fission (ΔE_{ST} and ΔE_{TT}). Singlet fission is a bimolecular process in which a molecule in the singlet ground state (S_0) interacts with a molecule in the first singlet excited state (S_1) to produce two molecules in the first triplet excited state ($T_1 + T_1$). A competing and unwanted for solar cell application process is the triplet–triplet annihilation, in which two triplets interact to produce a higher in energy triplet excited state (T_2). Thermodynamically, singlet fission will be the dominant process if the first feasibility condition $\Delta E_{ST} \lesssim 0$ and the second feasibility condition $\Delta E_{TT} < 0$ are both satisfied

fission is both thermodynamically favorable and competes effectively with other deactivation pathways. In reality, satisfying both provisions simultaneously is challenging, as it demands a delicate balance between singlet and triplet excitation energies — making proficient singlet fission materials exceptionally rare. Furthermore, to harvest the maximum of the solar irradiation, singlet fission chromophores must be characterized by a bright singlet excited state around 2 eV and, as a consequence of the first feasibility condition, with $E(T_1) \sim 1$ eV. Finally, to be implemented in a working solar cell, these molecules should be stable under ambient conditions and photoexcitation. In summary, compared to the voluminous group of conventional chromophores, only a small set of singlet fission chromophores is known and the structural variety within the set is relatively modest [5]. Advancement in the field can be achieved by collecting more evidence on the relationship between chemical structure and singlet fission propensity, as well as by exploring new strategies for molecular design. Moreover, the discovery of structurally diverse chromophores will extend the margins of crystal engineering and will allow for the fine tuneability of singlet fission propensity at the supramolecular level.

So far, several fruitful strategies for molecular design of singlet fission compounds have been reported, and one of the pioneers in the field was Prof. Masayoshi Nakano. In their seminal paper from 2011 "*Diradical character view of singlet fission*", Nakano and co-workers [6] demonstrated that open-shell molecules with low to intermediate diradical character (DRC) are among the best candidates that satisfy both feasibility conditions for singlet-to-triplets fission. Subsequently, the DRC-based design strategy inspired many scientists working in the field and gave rise to the discovery of new classes of singlet fission chromophores, composed mainly of doped or functionalized polycyclic aromatic/antiaromatic hydrocarbons (PAHs) [7–18]. Nakano's approach was even implemented in a high-throughput and machine learning-based large-scale screenings for new singlet fission compounds [19, 20].

Another fundamental strategy for the design of singlet fission molecules rooted in Baird's excited state aromaticity [21, 22] was recently demonstrated by Bronstein and Ottosson [23–25]. Baird's rule states that the T_1 energy decreases when 4n π-electron cycles are formed in the excited state, i.e., 4n π-electron cycles are deemed aromatic in the excited state. For some chromophores, Baird's rule applies for the energy of both the S_1 and T_1 excited states. By using Baird's aromaticity rule, several new singlet fission materials have been proposed, such as indolonaphthyridine thiophenes, Cibalackrot-type compounds, and fulvene derivatives.

In this study, we model new dimers of N-heterocyclic carbenes (NHC) and explore their singlet fission potential in terms of DRC and Baird's excited state aromaticity. The choice of compounds is inspired by the recently confirmed singlet fission proclivity of cyclic (alkyl)(amino)carbene (CAAC) dimers [26–28] and boron-doped PAHs [8]. The design strategy in the case of CAAC dimers is based on covalently bonded carbene units via π-conjugated cumulenic bridges of different length and type. The study on boron-doped PAHs revealed that polycyclic systems with bridgehead boron atoms belonging to two adjacent rings satisfy both feasibility conditions and are expected to minimize the thermal losses in singlet fission. As an amalgam of these two

design approaches, the carbene based compounds proposed here consist of two NHCs linked by a carbon–carbon double bond, each containing a nitrogen atom shared by adjacent cycles. In the literature, such NHC dimers are also known as electron-rich olefins, tetraazafulvalenes, and organic electron donors [29, 30]. Therefore, beside the singlet fission aspect discussed here, NHC dimers represent attractive materials for catalysis and redox applications such as greenhouse gas reduction agents, organic field-effect transistors, and fluorescent materials [31].

Starting with a parent imidazo[1,5-*a*]pyridine-3-ylidene NHC dimer, we investigated the effect of topology, substituents type, symmetry, annulation, ground state diradical character, excited state aromaticity, conformation, and stereoisomerism on the singlet fission propensity of the NHC dimers. In addition, we constructed analogues of NHC dimers, the so-called "locked" dimers, whose conformation is fixed by insertion of methylene latches with different length between the two non-shared nitrogens. The newly proposed compounds were employed as potent molecular tinkertoys, revealing new facets of the intricate relationship between structure and singlet fission propensity. Accounting for the large molecular size and the importance of both static and dynamic correlation effects, in this study we proposed a new protocol using simplified quantum chemistry (sQC) approaches [32] as screening tools for finding new singlet fission materials among NHC dimers and their analogues. The choice of computational sQC schemes was justified by performing benchmark studies with respect to high-level computational methods. To our knowledge, this is the first study, which demonstrates in detail the effect of such a wide list of structural factors on the excited state properties, as well as the relatively good performance of sQC approaches as computational screening tools in the singlet fission domain.

The paper is organized as follows. Section "Computational protocol" summarizes the main theoretical and computational aspects of ground state and excited state calculations. Section "Results and discussion" presents and discusses the excited state design of symmetric NHC dimers and their analogues, as well as of asymmetric NHC dimers. Details about the benchmark of the sQC method are provided in the Supplementary information (SI). Conclusions and perspectives in singlet fission aspect are drawn in the section "Summary".

Computational protocol

A brief summary of the computational protocol is presented in Scheme 2.

Excited state calculations

We start with the description of the computational procedure for evaluating the energies of the excited states, since the method and basis set for the ground state optimization were selected based on the benchmark results for the excited states. The singlet and triplet excitation energies and the first feasibility condition (ΔE_{ST}) for the NHC dimers were

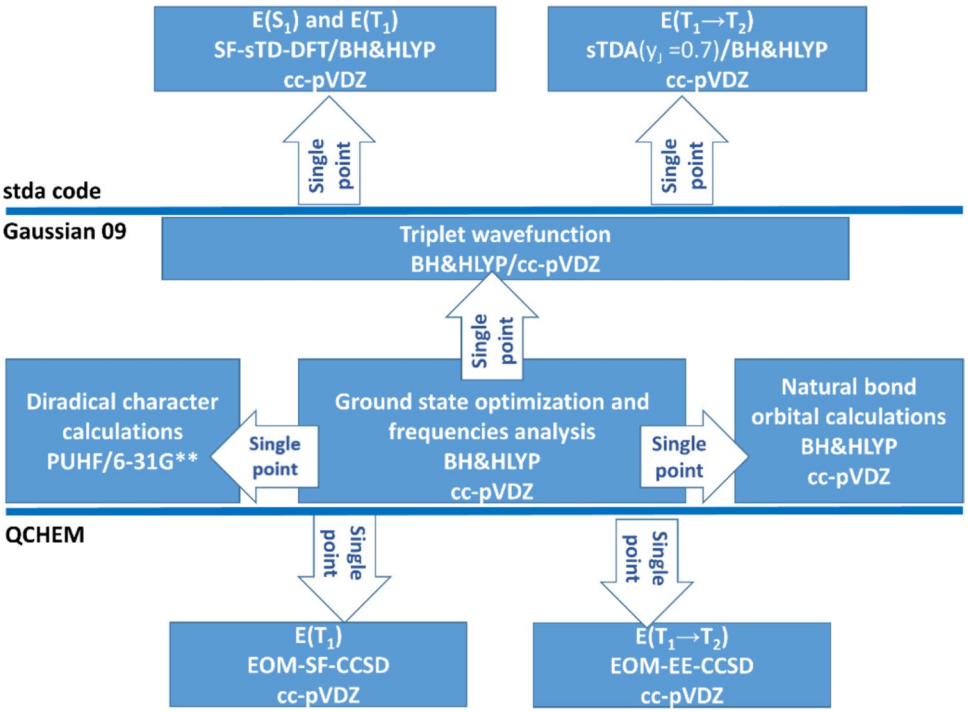

Scheme 2 Brief overview of the computational protocol described in the manuscript and in the supplementary information (SI). For the benchmark study aug-cc-pVDZ and cc-pVTZ additional basis sets were also used

evaluated with the spin-flip simplified time-dependent density functional theory (SF-sTD-DFT) approach [32–34]. This method is a simplification of the popular spin-flip time-dependent density functional theory (SF-TD-DFT) method [35–38] that follows the spin-flip scheme introduced by Krylov et al. [39–43]. The spin-flip formalism recovers a part of the static correlation missing in single reference methods by including one doubly excited configuration, thereby enabling an accurate description of open-shell systems such as diradicals. In the simplified version of the SF-TD-DFT method, considering the Tamm-Dancoff approximation and only collinear exchange–correlation (XC) functionals, the $\left(i_\alpha j_\alpha | a_\beta b_\beta\right)$ two-electron integrals between α occupied *i* and *j* and β unoccupied *a* and *b* molecular orbitals are approximated by short-range damped Coulomb interactions of transition density monopoles:

$$\left(i_\alpha j_\alpha | a_\beta b_\beta\right)' = \sum_A^N \sum_B^N q_{i_\alpha j_\alpha}^A q_{a_\beta b_\beta}^B \Gamma_{AB}^{\alpha\to\beta}$$

where $q_{i_\alpha j_\alpha}^A$ and $q_{a_\beta b_\beta}^B$ are transition charges obtained from a Löwdin orthogonalization and the Mataga – Nishimoto – Ohno – Klopman (MNOK) short-range damped Coulomb operator is [44–46]:

$$\Gamma_{AB}^{\alpha\to\beta} = \left(\frac{1}{\left(R_{AB}\right)^{y_{\alpha\to\beta}} + \left(1.4 a_x \eta\right)^{-y_{\alpha\to\beta}}} \right)^{\frac{1}{y_{\alpha\to\beta}}}$$

where R_{AB} is the interatomic distance between atoms A and B, a_x is the amount of Hartree–Fock exchange into the global hybrid exchange–correlation functional, η is the difference in the chemical hardness values of atoms A and B. The $y_{\alpha\to\beta}$ is a globally parametrized function of the amount of exact exchange a_x in the XC functional:

$$y_{\alpha\to\beta} = a_x + 0.3$$

This parameter was globally optimized for a benchmark set of nine diradicals [33] and further tested on other diradical systems to reproduce experimental UV–vis spectra considering expanded indenofluorenes analogues and diindeno[*n*]thiophene derivatives [34]. In addition, the space of single excitations is truncated according to a single energy threshold (E_{thresh}) that represents the spectral range from 0 to E_{thresh} eV. These approximations drastically reduce the computational cost while retaining most of its accuracy [33]. The default value of $E_{thresh} = 7.0$ eV was used all along this study. The transition dipole moments between the SF states obtained at the SF-sTD-DFT level of theory were multiplied by a factor of $\sqrt{2}$ to correct for the missing excitation in the α space [33].

To estimate the excitation energy $E(T_2)$, the same high-spin triplet reference was employed to calculate the vertical excitation energies $T_1 \to T_2$ with the unrestricted simplified time-dependent density functional theory using the Tamm-Dancoff approximation (UsTDA) [47, 48]. The $T_1 \to T_2$ energy difference was then added to $E(T_1)$ to approximate the vertical excitation energy $S_0 \to T_2$, i.e., $E(T_2)$. Thereafter, the second feasibility condition ΔE_{TT} was also estimated by using the combination of both the SF-sTD-DFT and UsTDA schemes.

As stated above, in the present study, the combination SF-sTD-DFT/UsTDA is particularly useful for screening big sets of large molecular size compounds because they provide better treatment of the spin symmetry compared to the conventional unrestricted DFT method and feature a high accuracy-to-computational-cost ratio. However, as it is the first time that the SF-sTD-DFT and UsTDA methods are employed to describe NHC dimers, we benchmarked the SF-sTD-DFT/UsTDA approaches against the high-level equation-of-motion spin-flip coupled-cluster method with single and double substitutions (EOM-SF-CCSD) and EOM-EE-CCSD to validate their applicability in this context [37, 39, 49, 50]. We also checked whether the default value of the parameters in SF-sTD-DFT/UsTDA methods were suitable for this class of compounds or if they needed any adjustment. A detailed discussion on the benchmark results for the SF-sTD-DFT/UsTDA approaches can be found in the Supplementary Information (SI).

The excited states calculations with the sQC approaches were performed with the BH&HLYP functional [51] and cc-pVDZ [52] basis set by using the optimized singlet ground state geometries. The SF-sTD-DFT computations were carried out with the default $y_{\alpha\to\beta}$ parameters. The UsTDA calculations were performed considering $y_J = 0.7$ in the damping MNOK function for approximated Coulomb integrals. All SF-sTD-DFT/sTDA results were obtained with the open-access *std2* program formerly known as *stda* code [53]. The Q-CHEM 5.1 [54] program package was used to obtain high-level EOM-SF-CCSD and EOM-EE-CCSD results for the benchmarks. The natural transition orbitals (NTOs) from the spin-flip calculations were visualized by using the JMol program [55].

It is important to note that in conventional TD-DFT and most molecular systems, the first excited singlet state (S_1) is typically the lowest-energy excitation with non-zero oscillator strength. In contrast, within the SF-sTD-DFT framework, the low-lying excited states often exhibit mixed character due to significant double excitations contributions. As a consequence, such lowest-energy singlet-like states may be optically dark and strongly spin-contaminated, which makes their direct identification as S_1 ambiguous and hampers their excited state character assignment. On the other hand, multi-configurational calculations on diradicaloids and singlet fission chromophores have shown that such systems may naturally possess a dark S_1 state with double excitation character [56]. Moreover, despite being optically dark, these

doubly excited states can be highly beneficial for singlet fission [57]. Therefore, in this work the S_1 state is defined as the lowest energy singlet-like excitation and in cases where the lowest-energy state is optically dark ($f \leq 0.0200$), the next higher-lying bright state was considered, namely S_2. The first feasibility condition is therefore calculated with respect to both S_1 and S_2. The raw data for the excitation energies, oscillator strengths and $<\hat{S}^2>$ values for the first four states of the dimers, obtained with the SF-sTD-DFT approaches, are summarized in a separate file (SI).

Ground state calculations and generation of a high-spin triplet reference function

Once the excited-state methods were verified, we followed a standard computational protocol for the sQC calculations. The ground state geometries of the NHC dimers were optimized with the BH&HLYP method and cc-pVDZ basis set without any symmetry constraints. All optimized structures were confirmed minima on the potential energy surface by vibrational frequencies analysis.

To quantify the delocalization effects in the different isomers, we have also performed second order perturbation energy calculations in a natural bond orbitals (NBO) basis set [58]. This allowed us to estimate the donor–acceptor stabilization energy, E(2), associated with $i \rightarrow j$ delocalization for configurations, where the NBO donors (i) are the lone pairs of the nitrogen atoms and the NBO acceptors (j) are the antibonding π^*-orbitals of the nearby double C = C bonds.

The diradical character of all compounds was also estimated by using the spin-projected PUHF theory [59] and the UNO/6-31G** method [60]. In the spin-projected PUHF theory, the diradical character (y_0, i = 0) related to HONO and LUNO can be calculated as:

$$y_i = 1 - \frac{2T_i}{1 + T_i^2}$$

where T_i represents the overlap integral between the corresponding orbital pairs. T_i is estimated from the UHF natural orbitals occupational numbers (n):

$$T_i = \frac{n_{HONO-i} - n_{LUNO+i}}{2}$$

For the diradical character, the spin-projected PUHF calculations were performed with UHF/6-31G** on top of the BH&HLYP optimized geometries.

The optimized ground state geometries at the BH&HLYP/cc-pVDZ level were used to generate high-spin triplet reference functions for the excited state calculations with the SF-sTD-DFT/sTDA methods.

All ground state simulations and generation of the high-spin triplet reference functions were performed with the Gaussian 09 software [61].

Results and discussion

NHC homodimers

Stereochemistry effects

Figure 1 shows the possible isomers of the parent NHC dimer, ***s*P**, and the free energy difference from the most

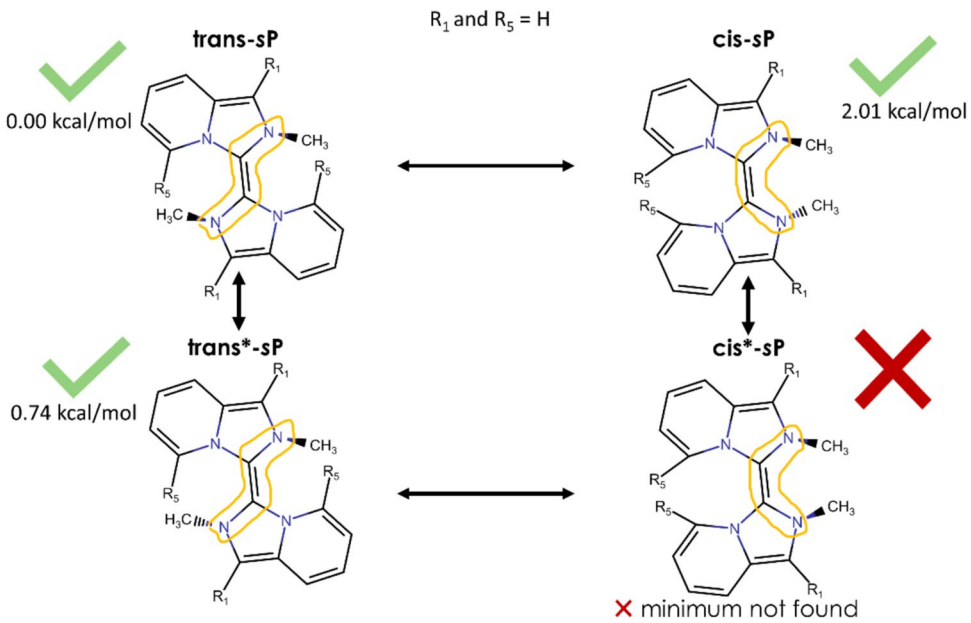

Fig. 1 Isomers in the parent NHC dimer ***s*P** (prefix *s* stands for "symmetric", i.e., homodimer) with respect to stereochemical configuration of the methylated nitrogens. Free energy difference (ΔG, kcal/mol) from the most stable isomer estimated at the BH&HLYP/cc-pVDZ level of theory

stable form. As illustrated on Fig. 1, the *cis–trans* isomerization around the exocyclic double bond in the NHC dimers triggers a change in the nitrogen stereochemical configuration. The conformational switch in stereochemical configuration is intensively used in the design of the first-generation molecular motors [62] based on overcrowded alkenes but it is rarely discussed in the area of NHCs or tetraazafulvalenes. Indeed, in our NHC dimers, each nitrogen is connected to four different structural fragments, one of which is the nonbonding electron pair. Assuming that the bridgehead nitrogens have less structural freedom, we concentrate on the methylated ones. Like this, with respect to stereochemical configuration of the methylated nitrogen, the parent NHC homodimer denoted as ***s*P** has four isomers (Fig. 1). Among them we were able to optimize only three forms (Fig. 1) — one *cis* (***cis*-*s*P**) and two *trans* (***trans*-*s*P** and ***trans**-*s*P**), suggesting that there is a strong steric hindrance of the CH_3 groups in the other ***cis**-*s*P** isomer.

Table 1 contains the results for the excitation energies, feasibility conditions, ground state geometry, and DRC of the studied symmetrical NHC dimers. For the parent ***s*P** homodimer, we observe a variation in the singlet fission propensity as a function of the molecular conformation and the stereochemical configuration of the methylated nitrogen atoms. Among the three isomers, ***cis*-*s*P** possesses the lowest-energy excited states and lowest values of the feasibility conditions, followed by the ***trans*-*s*P** and ***trans**-*s*P** forms. The variation in the excited states energies resulting from the stereoisomerism of ***s*P**, ***trans*** or ***trans****, is estimated to be ca. 0.3 eV for S_1, 0.38 eV for T_1, and 0.18 eV for T_2. On the other hand, the excited state energy differences between the ***cis*** and ***trans*** conformations of ***s*P** are ca. 0.3 eV for S_1, 0.26 eV for T_1, and 0.12 eV for T_2. Consequently, in the ***s*P** series of isomers, the first and second feasibility conditions vary broadly in the ranges 0.70–1.38 eV and 0.25–1.25 eV, respectively. Despite this variation, the feasibility conditions remain highly endothermic for spontaneous singlet fission. The latter agrees with the ground state DRC values (Table 1) for the three ***s*P** stereoisomers, which classify them as weak diradicaloids: 0.077 (***trans**-*s*P**), 0.111 (***cis*-*s*P**), and 0.097 (***trans*-*s*P**). And although the feasibility conditions are positive and correspond to unfavorable singlet fission processes, the stereoisomerism-driven strategy for molecular design deserves to be explored in more detail. Moreover, the results for the ***s*P** isomers reveal that in these systems small differences in DRC can lead to significant changes in the singlet fission propensity.

To explain this rather unexpected stereochemical effect on the exited states energies, we analyzed the NBO population, dihedral angles and bond lengths. These results for the parent compounds are summarized in Fig. 2. All these data reveal that the structures of the ***s*P** isomers differ from one another and that their conjugation pattern depends on the nitrogen stereochemistry. Regarding the structural aspect, the ***trans**-*s*P** isomer stands out because it is the only one possessing an inversion center in the middle of the exocyclic C = C bond (C_i point group), with the lone pairs of the methylated nitrogens oriented in opposite directions. Moreover, only in the ***trans**-*s*P** form, the torsion angle between the dimer's moieties is 180°, and its C = C exocyclic double bond is the shortest among all the isomers (Fig. 2). Consistent with the second-order perturbation analysis in NBO basis, in ***trans**-*s*P** the total charge transfer from the nitrogen lone pairs to the π*-orbital of the exocyclic C = C bond is weaker (~ 88 kcal/mol) and therefore this bond retains its bonding character to highest extent (Fig. 2). As a result of the discussed electronic structure, ***trans**-*s*P** possesses the highest excited states energies and the highest value of the first feasibility condition (Table 1). On the other hand, ***cis*-*s*P** is characterized with a torsion angle of 22° between the two moieties of the dimer and the longest C = C exocyclic bond. In ***cis*-*s*P**, the total donation from the nitrogen lone pairs to the π*-orbital of the exocyclic C = C bond is larger (~ 118 kcal/mol), which increases its antibonding character and the distance between the dimer's moieties. Consequently, the ***cis*-*s*P** form has the lowest in energy excited states and the smallest in value first feasibility condition. Finally, in structural aspect, ***trans*-*s*P** is very similar to ***cis*-*s*P**, since both isomers belong to the C_2 point group. Following the structure-properties correlation, the singlet fission properties of these isomers are also very close. It is interesting to note that despite the negligible steric hindrance of the methyl groups in the ***trans*-*s*P** form, the dihedral angle between the dimer's moieties is just 2° smaller than in the ***cis*-*s*P** form and the exocyclic C = C bond is slightly shorter. This structural similarity emphasizes further the role of the nitrogen stereochemical configuration for the conjugation pattern and for the singlet fission propensity of the NHC dimers.

Here, it is also important to note that the NBO analysis for all three ***s*P** forms suggests that the conjugation effects coming from $N(CH_3)$ are more pronounced. The second-order perturbation energy term associated with donation from the lone pairs of $N(CH_3)$ almost doubles going from ***trans**** to ***cis*** isomer. The more prominent role of the $N(CH_3)$ atoms is reasonable since they have more flexibility than the bridgehead nitrogens and can finely adjust the planarization within the heterocycles.

Substituent and annulation effects

Following the analysis of the stereochemical effects, we explored the role of the substituents. Starting from the isomers of the parent ***s*P** compound, we designed new functionalized NHC homodimers (Table 1 and Fig. 3). From a synthetic point of view, possible active positions for

Table 1 Symmetrical NHC dimers: energies [eV] of the: vertical excitation to the first and second singlet-like excited states $E(S_1/S_2)$, first triplet $E(T_1)$ and second triplet $E(T_2)$ excited states; oscillator strengths *f* for the $S_0 \rightarrow S_n$ transition; first ΔE_{ST} and second ΔE_{TT} singlet fission feasibility conditions [eV]; bond length of the exocyclic carbon–carbon bond R [Å]; dihedral angle Θ [°] between the carbene moieties, and diradical character (DRC). The molecular geometries were optimized at the BH&HLYP/cc-pVDZ level. The excited state results were obtained with the DFT using the SF-sTD-DFT/UsTDA approaches. In cases where the lowest-energy singlet-like state S_1 is optically forbidden ($f \leq 0.0200$), the corresponding characteristics of the lowest optically accessible higher-lying state (S_2) are additionally reported

Compound	Form	$E(S_1/S_2)$	*f*	$E(T_1)$	$E(T_2)$	ΔE_{ST}	ΔE_{TT}	Θ	R	DRC
***s*P**	***trans****	2.60	0.1749	1.99	2.73	1.38	1.25	180	1.346	0.077
***s*P**	***cis***	1.98	0.1288	1.34	2.43	0.70	0.25	22	1.353	0.111
***s*P**	***trans***	2.26	0.0001	1.61	2.55	0.96	0.67	160	1.349	0.097
		2.30	0.1788			0.92				0097
***s*P5-C≡CH**	***trans****	2.15	0.0000	1.74	2.19	1.33	1.29	180	1.352	0.132
		2.27	0.0974			1.21				
***s*P5-C≡CH**	***cis***	1.50	0.0000	0.97	1.86	0.44	0.08	34	1.359	0.183
		1.61	0.0975			0.33				
***s*P5-C≡CH**	***trans***	1.42	0.0001	1.08	1.73	0.73	0.42	145	1.359	0.173
		1.68	0.0954			0.48				
***s*P5-C≡N**	***trans****	2.08	0.0000	1.63	2.12	1.19	1.14	180	1.350	0.134
		2.18	0.0876			1.08				
***s*P5-C≡N**	***cis***	1.42	0.0000	0.84	1.80	0.26	−0.12	33	1.357	0.189
		1.49	0.0819			0.19				
***s*P5-C≡N**	***trans***	1.32	0.0001	0.96	1.63	0.61	0.30	146	1.358	0.176
		1.55	0.0790			0.73				
***s*P5-C≡C–C≡CH**	***trans****	1.89	0.0000	1.53	1.94	1.18	1.12	180	1.351	0.171
		2.05	0.0916			1.01				
***s*P5-C≡C–C≡CH**	***cis***	1.27	0.0001	0.76	1.61	0.25	−0.09	33	1.357	0.218
		1.38	0.0675			0.15				
***s*P5-C≡C–C≡CH**	***trans***	1.17	0.0006	0.88	1.44	0.58	0.31	145	1.359	0.212
		1.45	0.0721			0.30				
***s*P5-C≡C–C≡N**	***trans****	1.80	0.0000	1.44	1.86	1.09	1.02	180	1.350	0.171
		1.96	0.0794			0.92				
***s*P5-C≡C–C≡N**	***cis***	1.12	0.0002	0.61	1.49	0.10	−0.27	33	1.356	0.225
		1.23	0.0556			−0.01				
***s*P5-C≡C–C≡N**	***trans***	1.07	0.0009	0.77	1.34	0.48	0.21	146	1.358	0.176
		1.34	0.0590			0.21				
***s*P5-C≡C–C≡C–C≡CH**	***trans****	1.72	0.0000	1.41	1.79	1.10	1.03	180	1.351	0.197
		1.91	0.0939			0.91				
***s*P5-C≡C–C≡C–C≡CH**	***cis***	1.09	0.0003	0.62	1.41	0.15	−0.17	33	1.357	0.241
		1.22	0.0547			0.02				
***s*P5-C≡C–C≡C–C≡CH**	***trans***	1.00	0.0018	0.75	1.25	0.50	0.25	146	1.358	0.236
		1.31	0.0568			0.20				
***s*P5-C≡C–C≡C–C≡N**	***trans****	1.61	0.0000	1.31	1.70	1.01	0.92	180	1.350	0.199
		1.81	0.0855			0.81				
***s*P5-C≡C–C≡C–C≡N**	***cis***	0.94	0.0009	0.49	1.29	0.04	−0.31	32	1.356	0.247
		1.08	0.0447			−0.10				
***s*P5-C≡C–C≡C–C≡N**	***trans***	0.89	0.0030	0.65	1.15	0.41	0.15	146	1.357	0.239
		1.19	0.0455			0.11				
***s*P1-C≡CH**	***trans****	2.53	0.2229	1.95	2.59	1.37	1.31	180	1.345	0.106
***s*P1-C≡CH**	***cis***	1.89	0.1611	1.24	2.28	0.59	0.20	23	1.355	0.155
***s*P1-C≡CH**	***trans***	2.27	0.2310	1.60	2.49	0.92	0.70	160	1.348	0.129
***s*P1-C≡N**	***trans****	2.67	0.2314	2.05	2.76	1.43	1.34	180	1.343	0.072
***s*P1-C≡N**	***cis***	1.97	0.1657	1.27	2.37	0.57	0.17	23	1.354	0.132
***s*P1-C≡N**	***trans***	2.42	0.2422	1.70	2.66	0.97	0.73	159	1.347	0.093
***s*P1-C≡C–C≡CH**	***trans****	2.46	0.2971	1.91	2.50	1.36	1.32	180	1.345	0.147
***s*P1-C≡C–C≡CH**	***cis***	1.82	0.2037	1.18	2.17	0.54	0.19	24	1.356	0.203
***s*P1-C≡C–C≡CH**	***trans***	2.21	0.3046	1.56	2.41	0.91	0.71	160	1.348	0.173
***s*P1-C≡C–C≡N**	***trans****	2.52	0.3210	1.97	2.58	1.42	1.36	180	1.344	0.128
***s*P1-C≡C–C≡N**	***cis***	1.85	0.2207	1.17	2.19	0.50	0.15	24	1.356	0.194

Table 1 (continued)

Compound	Form	$E(S_1/S_2)$	*f*	$E(T_1)$	$E(T_2)$	ΔE_{ST}	ΔE_{TT}	Θ	R	DRC
***s*P1-C≡C–C≡N**	***trans***	2.27	0.3310	1.60	2.49	0.94	0.72	159	1.348	0.154
***s*P1-C≡C–C≡C–C≡CH**	***trans****	2.41	0.3826	1.88	2.42	1.35	1.34	180	1.344	0.178
***s*P1-C≡C–C≡C–C≡CH**	***cis***	1.77	0.2521	1.13	2.06	0.49	0.20	24	1.356	0.238
***s*P1-C≡C–C≡C–C≡CH**	***trans***	2.15	0.3896	1.52	2.34	0.90	0.71	159	1.349	0.206
***s*P1-C≡C–C≡C–C≡N**	***trans****	2.43	0.4283	1.90	2.43	1.37	1.37	180	1.344	0.171
***s*P1-C≡C–C≡C–C≡N**	***cis***	1.76	0.2825	1.11	2.04	0.46	0.18	24	1.357	0.239
***s*P1-C≡C–C≡C–C≡N**	***trans***	2.16	0.4379	1.53	2.35	0.91	0.72	159	1.349	0.201
***s*BP**	***trans****	1.80	0.1941	1.20	1.66	0.59	0.74	180	1.349	0.347
***s*BP**	***cis***	1.08	0.0028	0.39	1.52	−0.30	−0.74	24	1.364	0.444
		1.16	0.1418			−0.38				
***s*BP**	***trans***	1.38	0.0007	0.78	1.60	0.18	−0.04	159	1.357	0.398
		1.51	0.2314			0.06				

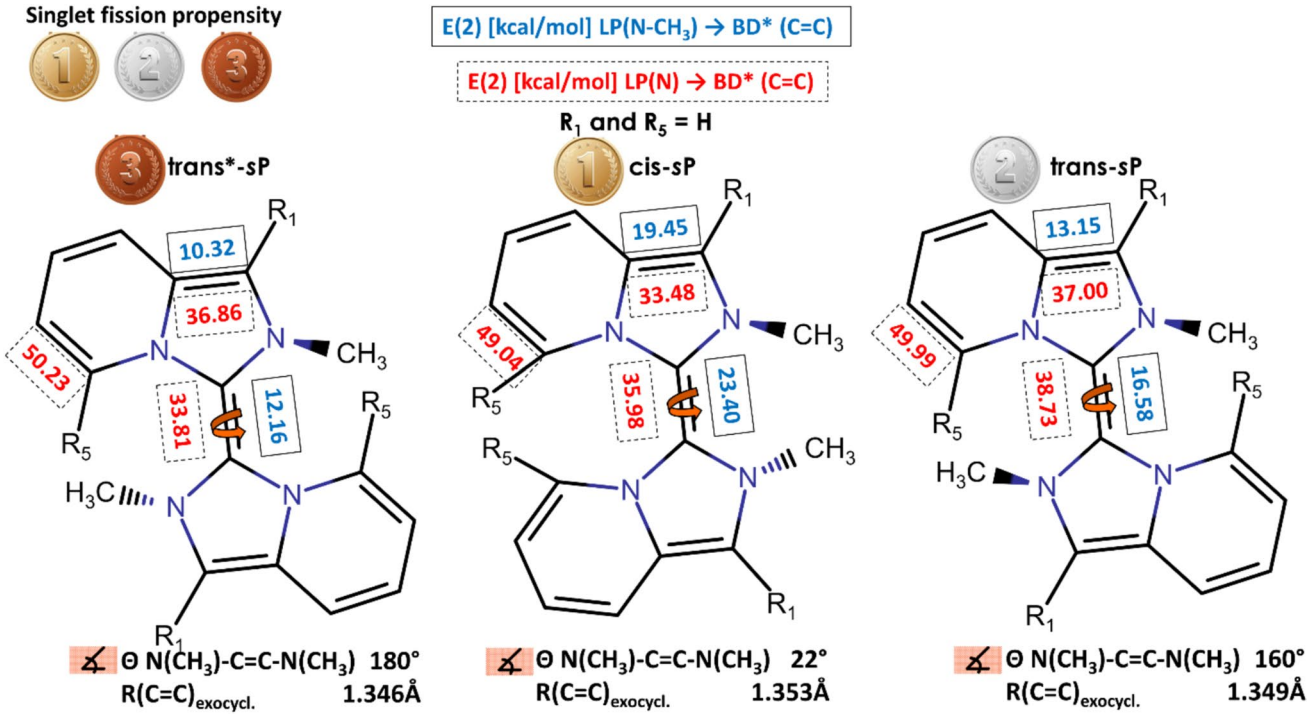

Fig. 2 Conjugation effects in the parent ***s*P** homodimer. NBO and second order perturbation theory analysis, E(2) [kcal/mol]: donations from the lone pairs of the N-CH_3 atoms (blue) and of the bridgehead N atoms (red) to the corresponding antibonding C=C double bonds. Bond length of the exocyclic C=C bond, R [Å], and key torsion angles, θ [°]. Ranking of the singlet fission propensity of the isomers. Only symmetry unique data are presented

substitution in ***s*P** are **1** and **5**. In principle, both π-donor and π-acceptor types of substituents can be introduced at these sites. However, according to Hückel's rule, the heterocycles in the parent NHC dimer contain an odd number of π-electrons and are thus non-aromatic. Consequently, it can be expected that symmetric substitution in the NHC dimers with π-donating substituents would destabilize the ground state by increasing the antiaromatic character of the imidazopyridine system, while π-withdrawing substituents would enhance its aromatic character. Therefore, all symmetrically functionalized NHC dimers proposed here accommodate π-acceptor type of substituents at the active positions. More precisely, we used π-electron-withdrawing groups containing -C≡N and -C≡CH linear fragments of varying conjugation length. The replacement of hydrogen atoms with larger substituents is motivated by the possibility for sterically driven twist around the exocyclic C=C bond, which is expected to stabilize the

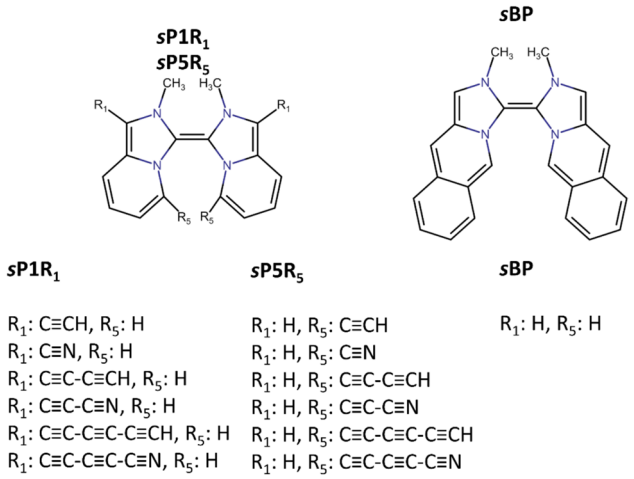

Fig. 3 Derivatives of the parent NHC homodimer, **sP**

diradicaloid form and to decrease the energy of the triplet excited state.

All tendencies discussed for the parent ***s*P** homodimers are conserved in their symmetrically substituted derivatives (Fig. 3 and Table 1). Namely, for a given dimer, the excited states energies and the values of the feasibility conditions again decrease in the order ***trans**-*s*P > *trans*-*s*P > *cis*-*s*P**, in line with an increase in the DRC. However, new excited state trends can be outlined for the substituted compounds. We found that the position of substitution is of paramount importance for the excited states properties and the singlet fission propensity of the NHC homodimers. This can be demonstrated with the introduction of the **-C≡N** group as a substituent, which is a relatively small and conformationally rigid strong acceptor. For example, when switching **-C≡N** position from **1** to **5**, the first and second feasibility condition for the dimers decreases by 0.2–0.4 eV. Obviously, this observation cannot be explained solely by the electronic properties of the substituents. The effect of the substituent's position on the excited state properties can be rationalized by the resonance structures and Baird's rule [22] (Fig. 4). Functionalization with an acceptor group at position **5** leads to a charge transfer from the $N(CH_3)$ nitrogen to the substituents, while attaching the same groups at position **1** causes a charge transfer from the bridgehead nitrogens to the substituents (**Fig. S6**, SI) When acceptor groups are attached to positions **1** of the dimer, both heterocycles become antiaromatic $(4n+2)$ in the excited state. On the other hand, the functionalization at positions **5** causes excited state antiaromatization limited only to the five membered rings. Therefore, in line with Baird's rule, the T_1 (and S_1) excited state energies are lower for the isomers functionalized at position **5** than for those substituted at position **1**. Along with these resonance effects, substitution at position **5** causes steric hindrance between the moieties of the dimers. As a consequence, compared with the unsubstituted ***s*P** dimer, the ***trans***- and ***cis***-forms functionalized at position **5** have larger torsion angle between the dimer's moieties (~ 33°) and longer exocyclic double bond (1.356–1.359 Å). Such a twist around the exocyclic bond is not induced by substituents introduced at position **1**. These structural results agree with the DRC values (Table 1), which show that the dimers functionalized at position **5** have higher DRCs than the corresponding dimers with substituents at position **1**. And here, we can conclude again that small differences in DRC cause significant changes in the singlet fission proclivity.

In addition to the effects of molecular topology, stepwise elongation of the π-conjugation of the substituents in the NHC homodimers stabilizes the triplet state and enhanes the singlet fission potential of the compounds.

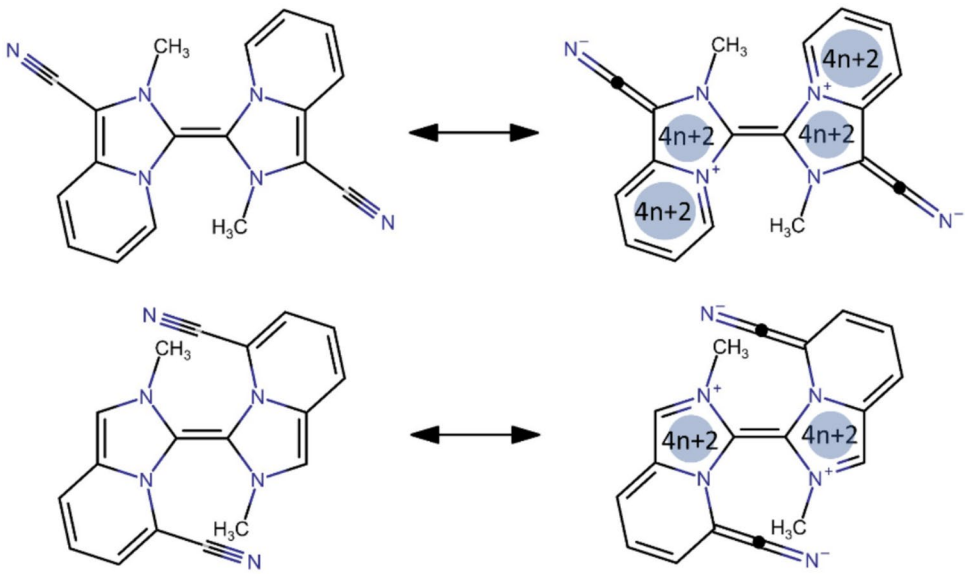

Fig. 4 Resonance structure of the ground (left) and excited (right) state in symmetric NHC dimers as a result of the substituent position and molecular topology

Among all substituted NHC homodimers, the smallest value of the first feasibility condition is predicted for ***cis-s*P5-C≡C–C≡C–C≡N**, being close to zero, which indicates the possibility for singlet fission without thermal losses. Actually, all ***cis-s*P** isomers functionalized at position 5 (except ***cis-s*P5-C≡CH**) should be prone to slightly endothermic singlet fission, as revealed by the ΔE_{ST} values below 0.25 eV. Moreover, for all these compounds the second feasibility condition is already exothermic. These results confirm again the potential of the stereisomerism-based design of singlet fission chromophores. The improvement in the singlet fission propensity of the dimers by substitution correlates well with the conjugation length of the substituent and hence, with the increase in the DRC values. For example, the unsubstituted ***cis-s*P** dimer has DRC of 0.111, while ***cis-s*P5-C≡N** and ***cis-s*P5-C≡C–C≡C–C≡N** possess DRC values of 0.189 and 0.247, respectively.

To explore the annulation effects, we modelled NHC homodimers of imidazoisoquinoline type (***s*BP**, Fig. 3). As shown in Table 1, annulation of ***s*P** has a favorable effect on the singlet fission propensity of the dimers. Indeed, ***cis-s*BP** becomes the first NHC homodimer with high singlet fission potential — it shows slightly exothermic ΔE_{ST} and exothermic ΔE_{TT}. Moreover, the ***trans-s*BP** is the first stereoisomer of this type with ΔE_{ST} value nearly zero and negative ΔE_{TT}. Such a strong annulation effect can be explained with an enhanced conjugation within the heterocycles at the expense of the exocyclic C = C bond as evidenced by the elongation of the latter. As a result, the DRC of the annulated forms is the highest in the series of homodimers, ~ 0.400 (Table 1), close to the DRC of the most promising singlet fission material — pentacene [6].

"Locked" analogues of NHC homodimers

Effect of the latch

Encouraged by the revealed structure-properties relationships discussed above, we constructed ***s*P** analogues "locked" in ***cis*** and ***cis**** conformations. Figure 5 shows the isomers of the "locked" dimers and the free energy difference from the most stable form. The locking of the dimers is ensured by the insertion of a latch between the non-shared nitrogen atoms, which is composed of two or three CH_2 groups. The design of "locked" analogues is motivated by the fact that the latch fixes the stereochemical centers in the NHC dimers. Here we were able to optimize three possible stereoisomers with respect to the methylated nitrogens (Fig. 5). We found that the most favorable unsubstituted "locked" dimer is ***cis*** in the case of the $-(CH_2)_2-$ latch, and ***cis**** when a $-(CH_2)_3-$ latch bridges the nitrogen atoms. Careful analysis of the molecular geometry reveals that the stronger steric hindrance between the methyl groups in the ***cis**** forms breaks the overall symmetry, which lowers the total energy of the systems. Thus, ***cis***-$(CH_2)_3$*s*P** belongs to the C_s point group, while ***cis*-$(CH_2)_2$*s*P** and ***cis*-$(CH_2)_3$*s*P** exhibit C_2 symmetry.

Results on the structure, vertical excitation energies, feasibility conditions, and DRC of the "locked" NHC homodimers are summarized in Table 2. The unsubstituted "locked" analogues are very similar to the ***cis-s*P** dimer, and the insertion of a latch between the nitrogen atoms has no strong impact on the DRC. Nevertheless, the first feasibility condition decreases slightly for ***cis***-$(CH_2)_3$*s*P** but not in the cases of ***cis*-$(CH_2)_2$*s*P** and ***cis*-$(CH_2)_3$*s*P**. This can be explained with the smaller degree of deplanarization

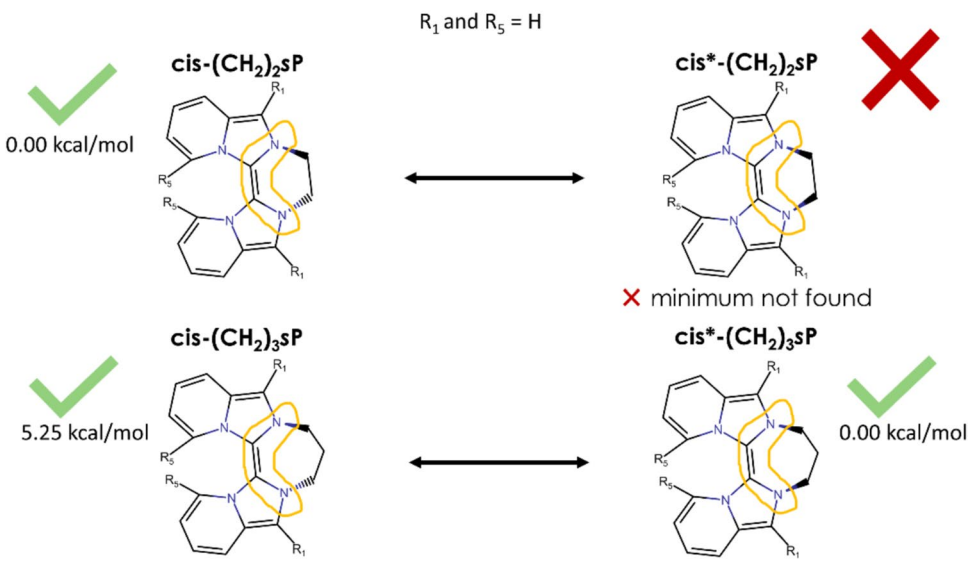

Fig. 5 Isomers of the "locked" analogues of the parent ***s*P** dimer: **$(CH_2)_2$*s*P** (top) and **$(CH_2)_3$*s*P** (bottom). Free energy difference ΔG [kcal/mol] from the more stable isomer estimated at the BH&HLYP/cc-pVDZ level of theory

Table 2 "Locked" NHC dimers: energies [eV] of the vertical excitation to the first and second singlet-like excited states $E(S_1/S_2)$, first triplet $E(T_1)$ and second triplet $E(T_2)$ excited states; oscillator strengths *f* for the $S_0 \rightarrow S_n$ transition; first ΔE_{ST} and second ΔE_{TT} singlet fission feasibility conditions [eV]; bond length of the exocyclic carbon–carbon bond R [Å]; dihedral angle Θ [°] between the carbene moieties, and diradical character (DRC). The molecular geometries were optimized at the BH&HLYP/cc-pVDZ level. The excited states results were obtained by using the SF-sTD-DFT/UsTDA approaches. In cases where the lowest-energy singlet-like state S_1 is optically forbidden ($f \leq 0.0200$), the corresponding characteristics of the lowest optically accessible higher-lying state (S_2) is additionally reported

Compound	Form	$E(S_1/S_2)$	*f*	$E(T_1)$	$E(T_2)$	ΔE_{ST}	ΔE_{TT}	Θ	R	DRC
$(CH_2)_2$*s*P	**cis**	1.87	0.0045	1.42	2.21	0.97	0.63	11	1.350	0.100
		1.99	0.0929			0.93				
$(CH_2)_2$*s*P5-C≡C–C≡C–C≡N	**cis**	1.01	0.0047	0.63	1.30	0.25	−0.04	17	1.354	0.208
		1.11	0.0329			0.15				
$(CH_2)_2$*s*BP	**cis**	1.05	0.0004	0.33	1.65	−0.39	−0.99	14	1.356	0.400
		1.21	0.0811			−0.55				
$(CH_2)_3$*s*P	**cis**	2.13	0.1057	1.55	2.42	0.97	0.68	15	1.348	0.092
$(CH_2)_3$*s*P5-C≡C–C≡C–C≡N	**cis**	1.27	0.0421	0.77	1.50	0.28	0.04	19	1.352	[a]NA
$(CH_2)_3$*s*BP	**cis**	1.29	0.1285	0.60	1.50	−0.08	−0.29	16	1.354	0.390
$(CH_2)_3$*s*P	**cis***	2.20	0.0975	1.39	2.74	0.58	0.04	25	1.353	0.092
$(CH_2)_3$*s*P5-C≡C–C≡C–C≡N	**cis***	1.33	0.0433	0.63	1.37	−0.07	−0.11	34	1.357	0.194
$(CH_2)_3$*s*BP	**cis***	1.29	0.0159	0.44	1.89	−0.41	−1.01	27	1.361	0.403
		1.38	0.0852			−0.50				

[a] Convergence problems in the broken-symmetry single point calculation

between the dimer's moieties in ***cis*-$(CH_2)_2$*s*P** and ***cis*-$(CH_2)_3$*s*P** (11°/15°). Figure 6 illustrates NBO population results for the "locked" analogues of the parent compounds. In all unsubstituted "locked" analogues, the total charge transfer stabilization energy from the nitrogen lone pairs to the π*-orbital of the exocyclic C = C bond is significant (≥ 110 kcal/mol), as in **cis-sP**.

Substituent and annulation effects

The substituted and annulated "locked" dimers designed here are represented in Fig. 7.

In general, the substituted "locked" compounds resemble their functionalized ***cis-s*P** analogues. This can be explained by the fact that in both series of derivatives there is a significant deplanarization of the dimer's moieties and identical elongation of the exocyclic C = C bond. For all three isomers, functionalization of the "locked" analogues with -C≡C–C≡C–C≡N groups at position **5** considerably lowers the values of the first feasibility condition below 0.28 eV and results in favorable values of the second feasibility condition (except ***cis*-$(CH_2)_3$*s*P5-C≡C–C≡C–C≡N**). In all cases, the functionalization effect is sufficiently strong to render singlet fission thermodynamically favorable — exothermic or slightly endothermic.

Further exploration of the molecular design strategies reveals that annulation has a positive impact on the singlet fission propensity of the "locked" analogues irrespective of the type of latch and nitrogens stereochemical configuration. When **$(CH_2)_2$*s*P** and **$(CH_2)_3$*s*P** are annulated, two possible singlet fission materials emerge, which satisfy both feasibility conditions. However, the annulation causes a significant unwanted decrease in the first feasibility condition, thus making ***cis*-$(CH_2)_2$*s*BP** and ***cis**-$(CH_2)_3$*s*BP** singlet fission candidates with thermal losses. All annulated "locked" homodimers possess DRC in the range of 0.390–0.400.

NHC heterodimers

In addition to the homodimers, we have also designed a set of asymmetrical NHC heterodimers (Figs. 8 and 9). Recently, Kozuch et al. demonstrated that asymmetric substitution in fulvalenes, which are to some extent similar to the NHC dimers, has a strong impact on both ground and excited state aromaticity [63]. Inspired by these findings, we applied a similar asymmetric design strategy and explored its effect on the singlet fission propensity of the NHC dimers. As substituents, we used $–OCH_3$ (π-donor) and –C≡N/–C≡C–C≡C–C≡N (π-acceptor). All feasible isomers with respect to the $N(CH_3)$ stereochemical configurations were simulated only in the case in which both donor and acceptor substituents are at position **5**, i.e., for ***as*P5OMeCN** (Fig. 8). It turned out that the most stable isomer of ***as*P5OMeCN** is of ***cis*** type, while both the ***trans*** and ***trans**** isomers are approximately 2 kcal/mol higher in energy.

Table 3 contains the results for the excitation energies, feasibility conditions, ground state geometry, and DRC of the studied asymmetric NHC dimers. The excited states

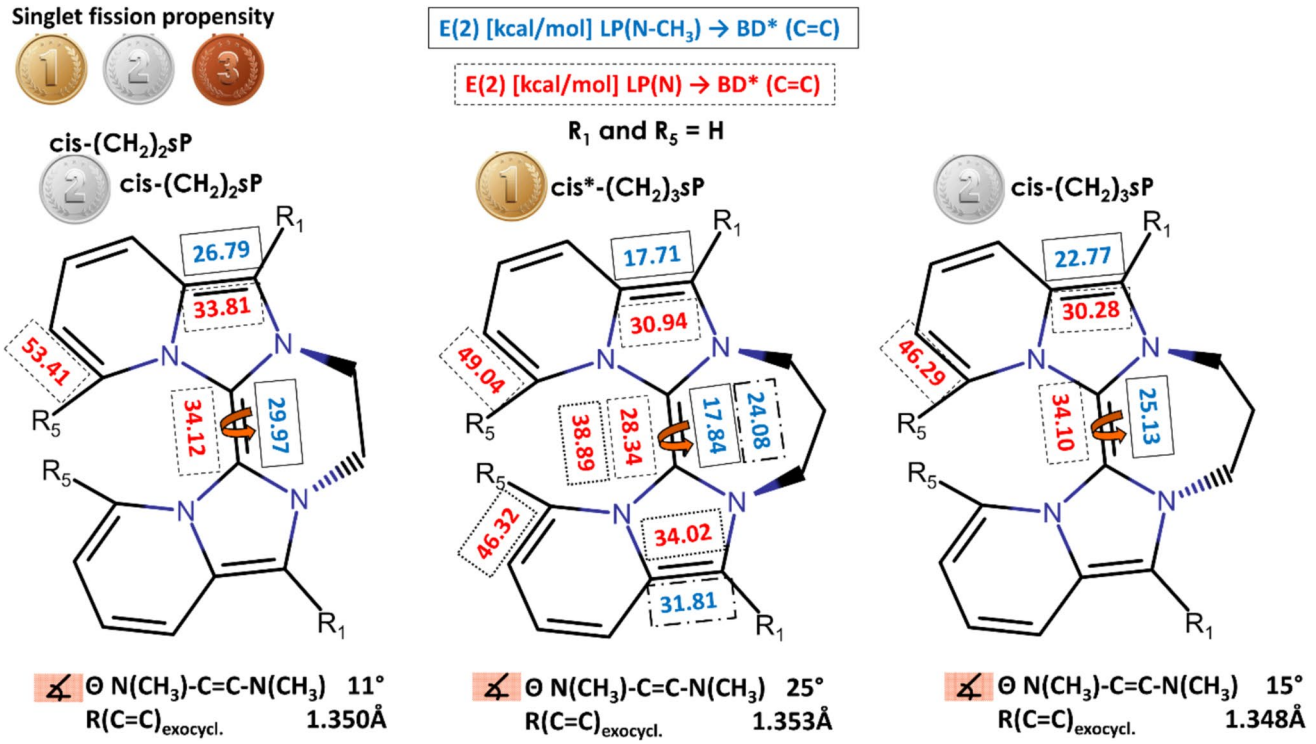

Fig. 6 Conjugation effects in the "locked" $(CH_2)_2$***s*****P** and $(CH_2)_3$***s*****P** homodimers. NBO and second order perturbation theory analysis, E(2) [kcal/mol]: donations from the lone pairs of the N-CH_3 nitrogens (blue) and of the bridgehead N-atoms (red) to the corresponding antibonding C = C double bonds. Bond length of the exocyclic C = C bond, R [Å], and key torsion angles, θ [°]. Ranking of the singlet fission propensity of the isomers. Only symmetry unique data are presented

results for the ***as*P5OMeCN** isomers confirm again the effect of stereoisomerism on the singlet fission propensity of NHC dimers. The ***trans**-*as*P5OMeCN** isomer is the least prone to singlet fission, while the ***cis*** and ***trans*** forms emerge as potential photovoltaic candidates. Figure 10 shows the NBO population and structural results for ***as*P5OMeCN**. The lack of singlet fission propensity for ***trans**-*as*P5OMeCN** is again in agreement with the structural results. Namely, the ***trans**** configuration of ***as*P5OMeCN** is characterized with a ~ 180° torsion angle between the dimer's moieties and the shortest exocyclic C = C bond. The NBO analysis also suggests weakest total donation (~ 86 kcal/mol) from the nitrogens' lone pairs to the π*-orbital associated with the exocyclic C = C bond in the case of ***trans**-*as*P5OMeCN**. Therefore, stereoisomers of ***trans**** type were not considered for the design of more asymmetric NHC dimers. On the contrary, the resonance stabilization in the case of ***cis/trans*-*as*P5OMeCN** is significantly higher (≥ 115 kcal/mol). This once again demonstrates that even in the absence of symmetry the stereoisomerism plays a significant role.

Logically, in the NHC heterodimers (Fig. 9), the conformational effects on the singlet fission propensity are even weaker. In fact, the excited state tunability in ***cis*/*trans*** NHC heterodimers is due to the different topology (Table 3). Longer exocyclic C = C bonds and more pronounced deplanarization between the dimer's moieties are observed for all heterodimers with acceptor groups at position **5**. Therefore, in agreement with the excited states results the following isomers: ***cis*/*trans*-*as*P5OMeCN, *cis*/*trans*-*as*P1OMe5CN**, ***cis*/*trans*-*as*P5CN**, and ***as*P1OMe5(CC)$_2$CN** appear as potential candidates for endothermic singlet fission. The values for the first feasibility conditions of the best heterodimers vary between − 0.18 and 0.07 eV, and in all cases the second feasibility condition is below zero and hence, favorable. In contrast, the introduction of the even bulkier –OCH_3 group at position **5** does not affect significantly the ground state structure and does not increase the singlet fission propensity. The importance of the acceptor at position **5** can be explained again with a charge transfer in the excited state and Baird's rule. The possible resonance structures for this compound are represented on Fig. 11. When the acceptor group is at position **5**, the excited state charge transfer is represented by a resonance structure containing one antiaromatic (4n + 2)-π and one aromatic (4n)-π heterocycle according to Baird's rule. The presence of an aromatic (4n)-π heterocycle in the excited state causes stabilization of the triplet in regard to the unsubstituted parent dimer ***s*P**, as well as with respect to the

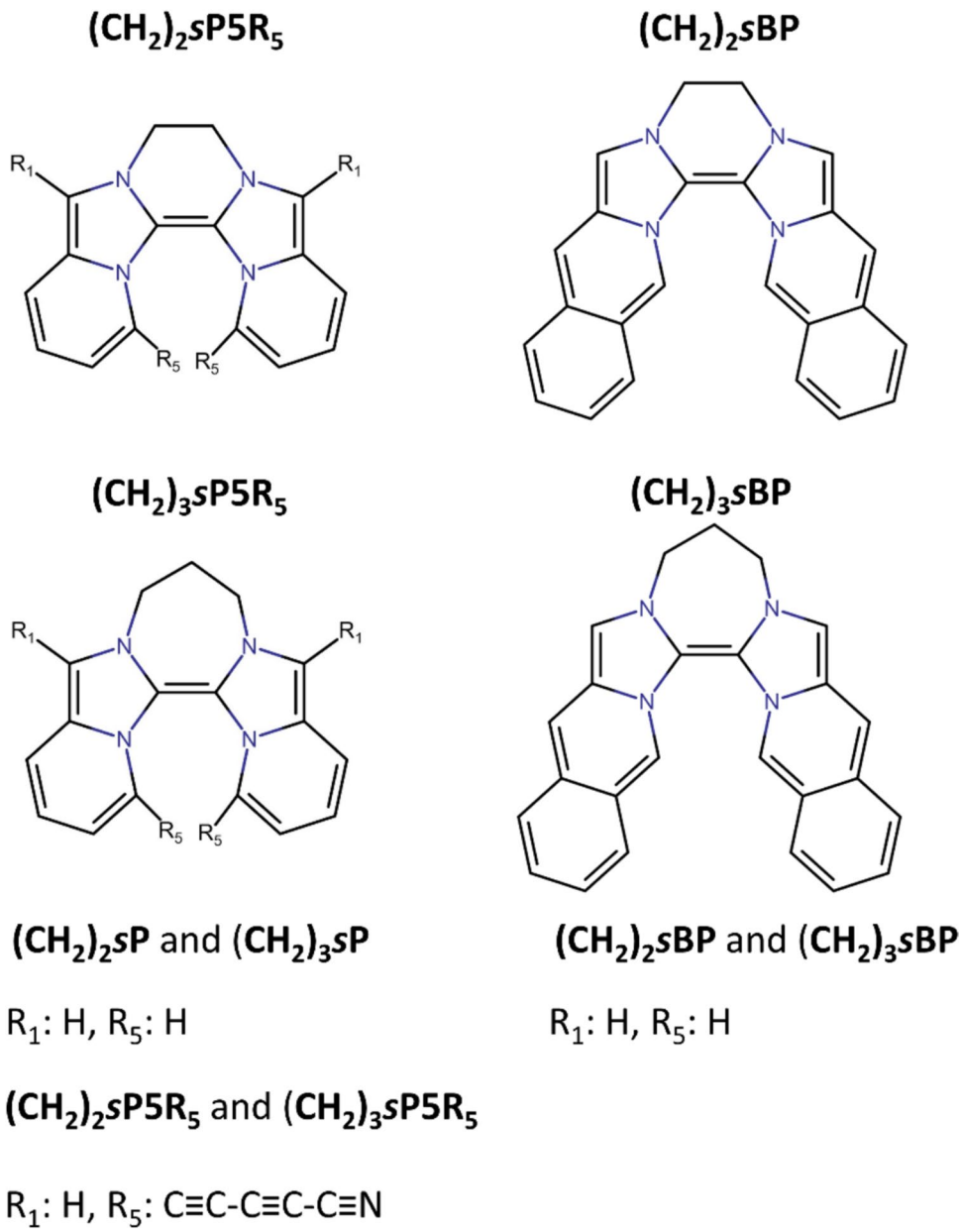

Fig. 7 Derivatives of the "locked" NHC homodimers, **$(CH_2)_2$sP** and **$(CH_2)_3$sP**

homodimer with acceptor groups at position **5**. Contrariwise, the attachment of an acceptor group at position **1** leads to an excited state resonance structure represented by one aromatic (4n)-π and two antiaromatic (4n + 2)-π heterocycles according to Baird's rule. The excess of antiaromatic (4n + 2)-π cycles destabilizes the excited state and has a negative impact on the singlet fission propensity of the heterodimer.

Comparison between the excited state results for mono- and disubstituted heterodimers, ***as*P5CN** and ***as*P5OMeCN,** reconfirms the role of the acceptor substituent at position **5**. These two dimers have identical and favorable singlet fission propensity. This suggests that the effect of a donor group on the excited state properties is negligible and hence, that an excited state charge transfer is not achievable. Indeed, molecular orbital analysis reveals that in the asymmetric NHC dimers, the HOMOs are delocalized, while the LUMOs are strongly localized on the dimer's moiety containing the acceptor substituent (Fig. S8, SI). Such a strong localization of LUMOs signifies a weak electron coupling between dimer's moieties. It is also in agreement with the relatively low DRC of the NHC homodimers despite their large π-conjugated system (Table 1), as well as with the lack of conformational effect on the singlet fission propensity in the case of heterodimers (Table 3).

Finally, from the perspective of photovoltaics application, we should discuss the absorption cross sections

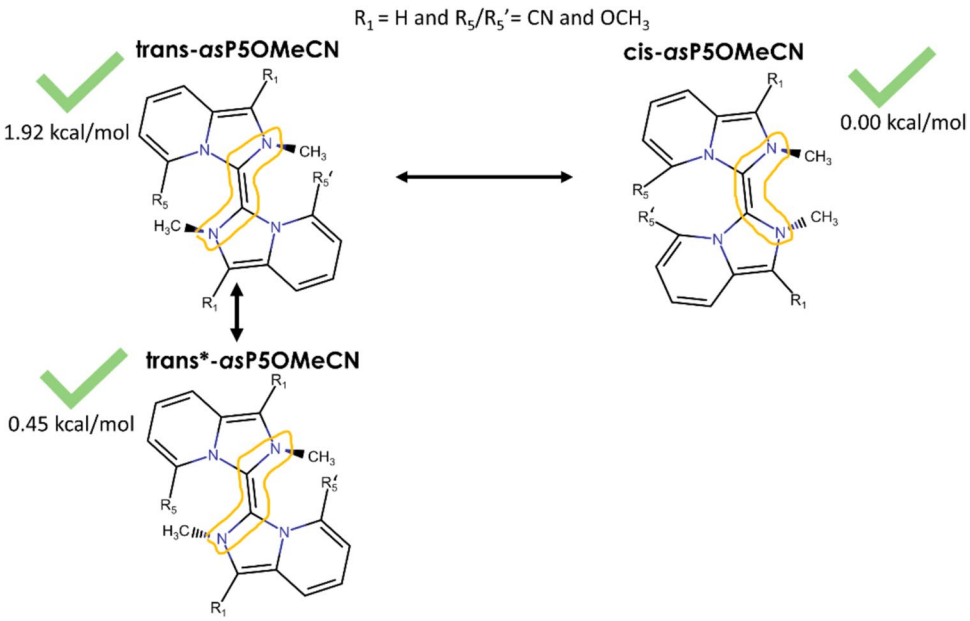

Fig. 8 Isomers of the heterodimer ***as*P5OMeCN**: free energy difference (ΔG, kcal/mol) from the most stable isomer estimated at the BH&HLYP/cc-pVDZ level of theory (prefix *as* stands for asymmetric, i.e., heterodimer)

for the best singlet fission candidates — ***cis-s*P5-C≡N, *cis-s*P5-C≡C–C≡CH, *cis-s*P5-C≡C–C≡N, *cis-s*P5-C≡C–C≡C–C≡CH, *cis-s*P5-C≡C–C≡C–C≡N, *cis-s*BP, *trans-s*BP, *cis*-$(CH_2)_2$*s*P5-C≡C–C≡C–C≡N, *cis**-$(CH_2)_3$*s*P5-C≡C–C≡C–C≡N, *cis/trans-as*P5OMeCN, *cis/trans-as*P1OMe5CN, *cis/trans-as*P1OMe5$(CC)_2$CN**, and ***cis/trans-as*P5CN**. The SF-sTD-DFT results for the symmetric unlocked dimers suggest "dark" S_1 excited states ($f \leq 0.0200$) lying in the NIR region. Such dark excited states are usually doubly excited, which, as demonstrated by Casanova, can be regarded as an advantage for singlet fission [57]. A more detailed investigation of the character and properties of doubly excited states would, however, require the use of multiconfigurational wavefunction methods and is therefore outside the scope of this study. Nevertheless, going beyond these "dark" excited state, all selected compounds absorb simultaneously in both the NIR (Table 1, 2, 3) and the UV–vis/near-UV region (Table 4). It can be speculated that the existence of a singlet fission material absorbing in both the NIR and UV–vis regions might ensure capturing of a broad range

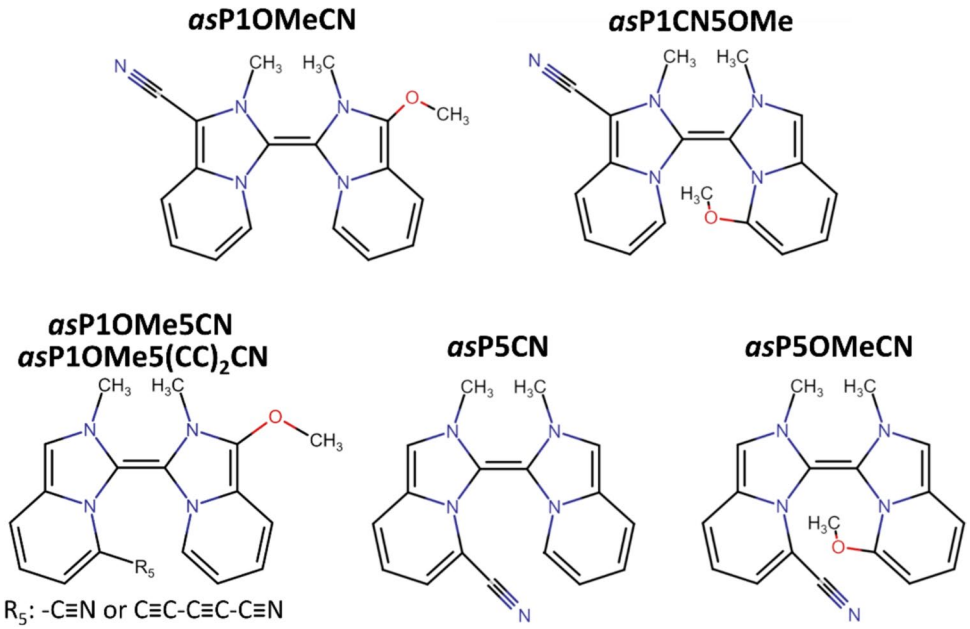

Fig. 9 Derivatives of the parent NHC homodimer with asymmetric substitution, i.e., NHC heterodimers, ***as*P**

Table 3 NHC heterodimers: energies [eV] of the vertical excitation to the first singlet $E(S_1)$, first triplet $E(T_1)$ and second triplet $E(T_2)$ excited states; oscillator strength f for the $S_0 \rightarrow S_1$ transition; first ΔE_{ST} and second ΔE_{TT} singlet fission feasibility conditions [eV]; bond length of the exocyclic carbon–carbon bond R [Å]; dihedral angle Θ [°] between the carbene moieties, and diradical character (DRC). The molecular geometries were optimized at the BH&HLYP/cc-pVDZ level. The excited states results were obtained with the DFT using the SF-sTD-DFT/UsTDA approaches

Compound	Form	$E(S_1)$	f	$E(T_1)$	$E(T_2)$	ΔE_{ST}	ΔE_{TT}	Θ	R	DRC
*as*P1OMeCN	***cis***	2.00	0.1357	1.29	2.60	0.57	−0.03	23	1.354	0.109
*as*P1OMeCN	***trans***	2.23	0.0956	1.62	2.12	1.00	1.11	159	1.350	0.097
*as*P5OMeCN	***trans****	2.14	0.0416	1.24	3.25	0.35	−0.76	176	1.351	0.110
*as*P5OMeCN	***cis***	1.53	0.0470	0.75	2.77	−0.02	−1.26	27	1.361	0.137
*as*P5OMeCN	***trans***	1.52	0.0438	0.76	2.76	0.00	−1.24	147	1.358	0.140
*as*P1OMe5CN	***cis***	1.52	0.0525	0.79	2.53	0.07	−0.95	25	1.353	0.146
*as*P1OMe5CN	***trans***	1.51	0.0757	0.70	2.42	−0.11	−1.03	151	1.356	0.157
*as*P1CN5OMe	***cis***	2.16	0.1215	1.35	2.91	0.54	−0.21	27	1.354	0.080
*as*P1CN5OMe	***trans***	2.11	0.1021	1.27	2.94	0.44	−0.39	150	1.359	0.091
*as*P5CN	***cis***	1.50	0.0546	0.77	2.47	0.04	−0.93	27	1.355	0.147
*as*P5CN	***trans***	1.56	0.0738	0.74	2.37	−0.07	−0.88	150	1.360	0.154
*as*P1OMe5$(CC)_2$CN	***cis***	1.11	0.0318	0.46	2.24	−0.18	−1.31	27	1.355	0.198
*as*P1OMe5$(CC)_2$CN	***trans***	1.13	0.0332	0.47	2.33	−0.18	−1.38	150	1.360	0.190

of wavelengths from the solar spectrum and this would have a positive impact on the solar cell efficiency. This strategy is already successfully implemented in conventional organic solar cells [64]. Moreover, all asymmetric dimers possess bright singlet excited state around 2 eV, corresponding to the maximum of the solar irradiation, which is another advantage of these compounds from photovoltaic standpoint.

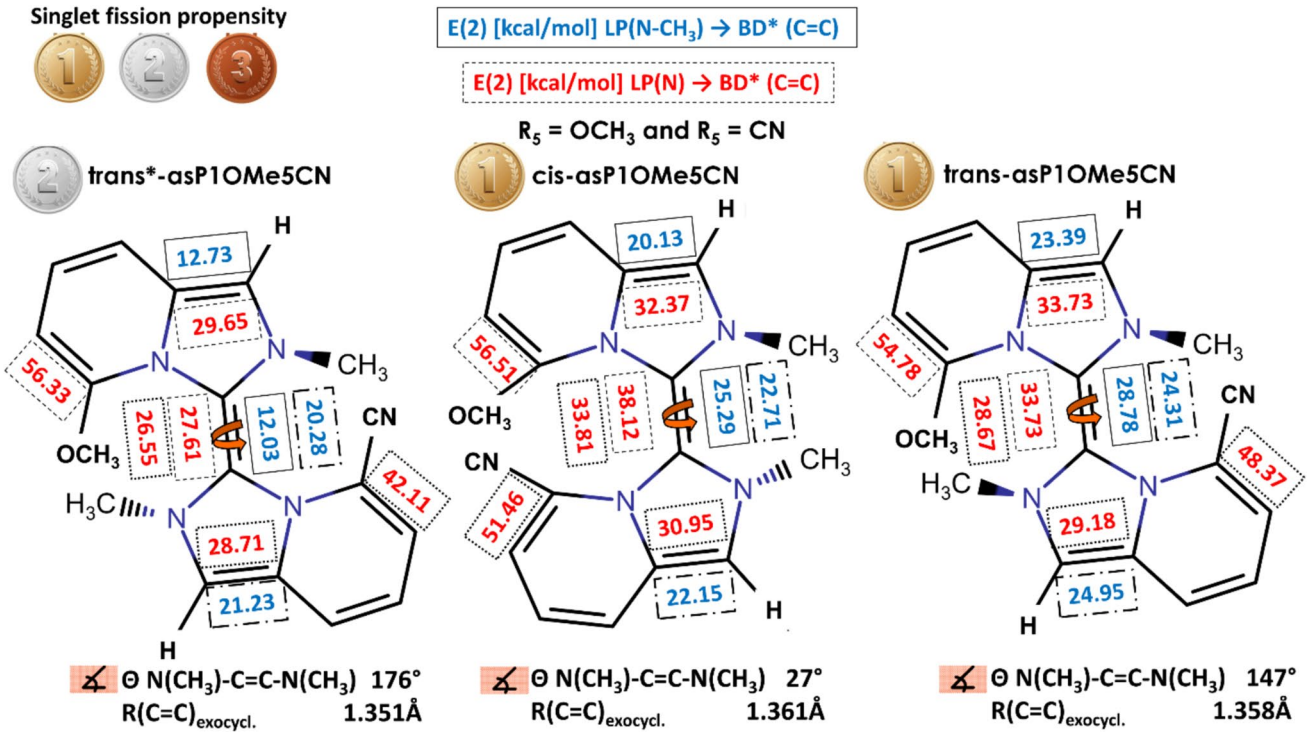

Fig. 10 Conjugation effects in the ***as*P5OMeCN** heterodimer. NBO and second order perturbation theory analysis, E(2) [kcal/mol]: donations from the lone pairs of the N-CH_3 atoms (blue) and of the bridgehead N-atoms (red) to the corresponding antibonding C=C double bonds. Bond length of the exocyclic C=C bond, R [Å], and key torsion angles, θ [°]. Ranking of the singlet fission propensity of the isomers

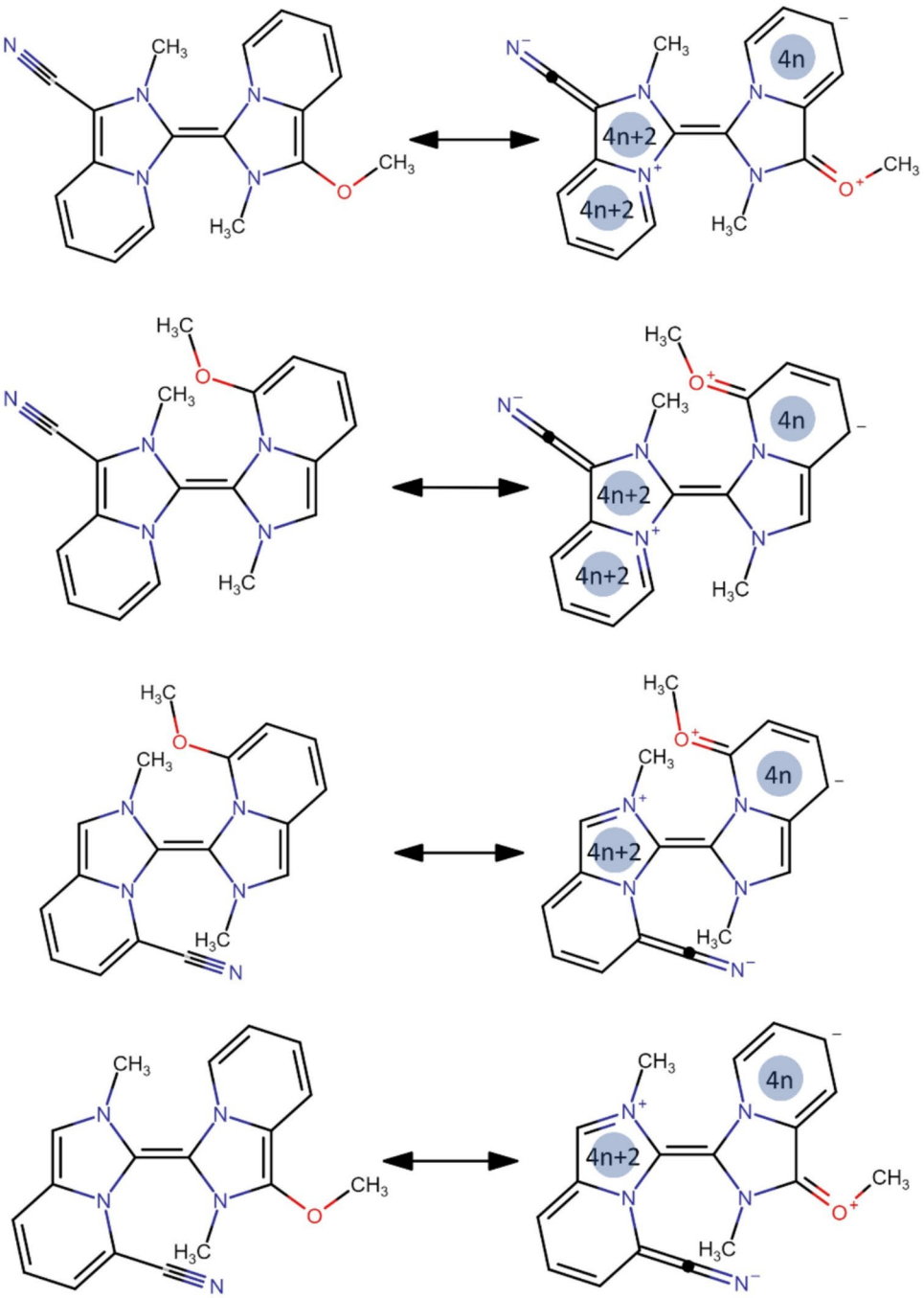

Fig. 11 Resonance structure in the ground (left) and excited (right) state in NHC heterodimers as a consequence of the molecular topology

Another aspect, which is important for the practical use of the selected candidates concerns their chemical reactivity, stability, and synthetic feasibility. From an experimental point of view, NHC homo- and heterodimers are usually obtained by a reaction between two free carbenes through the so-called Wanzlick equilibrium [65, 66]. Alternative synthetic routes include dechalcogenation of NHC thions or cleavage of a small molecule from a carbene derivative [67, 68]. They are prepared by heating of two different dimers. From a theoretical perspective , one of the factors related to the chemical reactivity is the diradical character. Our simulations reveal that all of the symmetric shortlisted compounds possess diradical characters of approximately 0.4, i.e., in this respect they are similar to the best-known singlet fission chromophore–pentacene. On the other hand, the diradical character of the asymmetric candidates varies between 0.1 and 0.2. Therefore, the demonstrated strategy for molecular design of singlet fission NHC dimers can be adapted to achieve the desired diradical character range.

Table 4 SF-sTD-DFT/cc-pVDZ results for the most intense UV–vis excitations of the best singlet fission candidates: $E(S_n)$ [eV] — excitation energy and *f* — oscillator strength

Compound	$E(S_n)^{UV/UV-vis}$	$f(S_n)^{UV/UV-vis}$
*cis-s*P5-C≡N	3.07	0.0233
cis-P5-C≡C–C≡CH	3.14	0.0392
cis-P5-C≡C–C≡N	3.06	0.0254
cis-P5-C≡C–C≡C–C≡CH	2.77	0.0255
cis-P5-C≡C–C≡C–C≡N	2.67	0.0197
cis-BP	2.97	0.0472
trans-BP	3.31	0.2233
cis-$(CH_2)_2$P5-C≡C–C≡C–C≡N	2.68	0.0325
*cis**-$(CH_2)_3$P5-C≡C–C≡C–C≡N	2.64	0.0212
*cis-as*P5OMeCN	2.43	0.0440
*trans-as*P5OMeCN	2.41	0.0298
*cis-as*P1OMe5CN	2.20	0.0296
*trans-as*P1OMe5CN	2.04	0.0168
*cis-as*P1OMe5$(CC)_2$CN	2.29	0.0422
*trans-as*P1OMe5$(CC)_2$CN	2.30	0.0361
*cis-as*P5CN	2.13	0.0236
*trans-as*P5CN	3.31[a]	0.0894

[a]There is a singlet excited state at 2.011 eV with an oscillator strength close to 0.02 (0.0144)

Summary

We have designed new NHC dimers and their "locked" analogues, which have the potential to serve as singlet fission chromophores in solar cells. The compounds represent versatile molecular tinkertoys, which allowed us to explore a variety of structure-properties relationships from a singlet fission standpoint, such as the individual or combined influence of the following factors: topology, type of substituents, symmetry (homo- and heterodimers), excited state aromaticity, conformation and stereoisomerism, annulation, and the length of the latch in the "locked" analogues. The study confirms many of the existing strategies for the design of singlet fission chromophores, for example the DRC-based approach, and reports for the first time the role of stereoisomerism for excited state tunability in these materials. As a result of the detailed analysis, seventeen promising singlet fission candidates are highlighted. Possible advantage of all shortlisted compounds is that they and absorb intensely in the NIR, as well as in the UV–vis/near UV regions. Moreover, most of the shortlisted candidates, in particular the asymmetric dimers, possess a bright excited state around 2 eV, which is around the maximum of the solar irradiation, and in the same time maintain a relatively low diradical character.

From a methodological point of view, we demonstrate for the first time the good performance of the sQC methods like SF-sTD-DFT and UsTDA for the screening of large in molecular size chromophores with potential photovoltaic application. The advantage of these sQC methods is that they offer a reasonable treatment of both static and dynamic correlation effects in diradicaloids at a low computational cost. In the era of big data [20], such excited state methods, which allow time-saving and reliable computational exploration of qualitative trends, will become more and more important. The screening procedure for qualitative estimation of the singlet fission propensity by means of the sQC methods should be followed by high-level quantum chemistry calculations on the shortlisted candidates for a quantitative assessment. In particular, sophisticated approaches should be applied to rationalize the singlet fission propensity at both molecular [8] and supramolecular level [69–71]. In principle, adiabatic excitation energies should also be investigated to confirm our theoretical predictions. However, at the current stage of development, excited-state geometry optimizations with SF-sTD-DFT are not feasible. Also, going beyond SF-sTD-DFT approach is challenging due to the molecular size of the proposed singlet-fission chromophores and their non-negligible diradical character.

Besides the singlet fission aspect discussed here, NHC dimers are compounds of much broader application and fundamental importance. For example, NHC dimers represent tetraazafulvalenes, which are building blocks in the design of super electron donors. In addition, they are also involved in the Wanzlick's equilibrium, which is a central problem in carbene chemistry. Moreover, among the investigated compounds not suitable for singlet fission there are also a few NHC dimers with a bright S_1 state and a closely lying T_1, which seem promising as thermally activated delayed fluorescent chromophores. Therefore, we believe that our results give new insights beyond the singlet fission realm.

Supplementary Information The online version contains supplementary material available at https://doi.org/10.1007/s00894-026-06774-9.

Acknowledgements The authors acknowledge the financial support of the Bulgarian National Science Fund, contract КП-06-H39/2 from 09.12.2019. The computational work is supported by project No. BG16RFPR002-1.014-0014-C01 "Development Program with a Business Plan for the Laboratory Complex of Sofia Tech Park", which is implemented under the "Research, Innovation and Digitalization for Smart Transformation" Program, co-financed by the European Union through the European Regional Development Fund. The authors would like to thank to Mrs. Gergana Kostadinova for her assistance with data collection during the initial stages of this research.

Author contribution J.R. conceived of the presented idea. M. de W. developed the code and refined the computational approach. R. L. guided the synthetically feasible molecular design. Data collection and results analysis were performed by J.S., A.T., M. de W., and J. R. The first draft of the manuscript was written by J.R. All authors reviewed and edited the manuscript, read and approved its final version.

Funding The authors acknowledge the financial support of the Bulgarian National Science Fund, contract КП-06-H39/2 from 09.12.2019. The computational work is supported by project No. BG16RFPR002-1.014–0014-C01 "Development Program with a Business Plan for the

Laboratory Complex of Sofia Tech Park", which is implemented under the "Research, Innovation and Digitalization for Smart Transformation" Program, co-financed by the European Union through the European Regional Development Fund.

Data availability No datasets were generated or analysed during the current study.

Declarations

Conflict of interest The authors declare no competing interests.

References

1. Shockley W, Queisser HJ (1961) Detailed balance limit of efficiency of p-n junction solar cells. J Appl Phys 32:510–519. https://doi.org/10.1063/1.1736034
2. Hanna MC, Nozik AJ (2006) Solar conversion efficiency of photovoltaic and photoelectrolysis cells with carrier multiplication absorbers. J Appl Phys 100:074510. https://doi.org/10.1063/1.2356795
3. Smith MB, Michl J (2010) Singlet fission. Chem Rev 110(11):6891–6936. https://doi.org/10.1021/cr1002613
4. Casanova D (2018) Theoretical modeling of singlet fission. Chem Rev 118(15):7164–7207. https://doi.org/10.1021/acs.chemrev.7b00601
5. Smith MB, Michl J (2013) Recent advances in singlet fission. Annu Rev Phys Chem 64:361–386. https://doi.org/10.1146/annurev-physchem-040412-110130
6. Minami T, Nakano M (2011) Diradical character view of singlet fission. J Phys Chem Lett 3(2):145–150. https://doi.org/10.1021/jz2015346
7. Zeng T, Ananth N, Hoffmann R (2014) Seeking small molecules for singlet fission: a heteroatom substitution strategy. J Am Chem Soc 136(36):12638–12647. https://doi.org/10.1021/ja505275m
8. Stoycheva J, Tadjer A, Garavelli M, Spassova M, Nenov A, Romanova J (2020) Boron-doped polycyclic aromatic hydrocarbons: a molecular set revealing the interplay between topology and singlet fission propensity. J Phys Chem Lett 11(4):1390–1396. https://doi.org/10.1021/acs.jpclett.9b03406
9. Zeng T, Mellerup SK, Yang D, Wang X, Wang S, Stamplecoskie K (2018) Identifying $(BN)_2$-pyrenes as a new class of singlet fission chromophores: significance of azaborine substitution. J Phys Chem Lett 9(11):2919–2927. https://doi.org/10.1021/acs.jpclett.8b01226
10. Ito S, Nakano M (2015) Theoretical molecular design of heteroacenes for singlet fission: tuning the diradical character by modifying π-conjugation length and aromaticity. J Phys Chem C 119(1):148–157. https://doi.org/10.1021/jp5103737
11. Nagami T, Miyamoto H, Yoshida W, Okada K, Tonami T, Nakano M (2020) Theoretical molecular design of phenanthrenes for singlet fission by diazadibora-substitution. J Phys Chem A 124(34):6778–6789. https://doi.org/10.1021/acs.jpca.0c05359
12. Nagami T, Okada K, Miyamoto H, Yoshida W, Tonami T, Nakano M (2020) Molecular design principle for efficient singlet fission based on diradical characters and exchange integrals: multiple heteroatom substitution effect on anthracenes. J Phys Chem C 124(22):11800–11809. https://doi.org/10.1021/acs.jpcc.0c02369
13. Moradas DR, Tang Y, Burnea FK, Li N, Lee JY (2024) Monosilicon derivatives of phenanthrene and pyrene as potential singlet fission materials for high-performance solar cells. J Phys Chem A 128(38):8159–8169. https://doi.org/10.1021/acs.jpca.4c04894
14. Mathew CM, Varghese A, Sugunan SK, Thomas VI (2022) Rapid computational approach towards designing singlet-fission chromophores by tuning the diradical character of heteroatom-doped polycyclic aromatic hydrocarbons using the atom-specific Fukui function. J Phys Chem A 126(10):1579–1590. https://doi.org/10.1021/acs.jpca.1c08094
15. Liu X, Tom R, Gao S, Marom N (2020) Assessing zethrene derivatives as singlet fission candidates based on multiple descriptors. J Phys Chem C 124(48):26134–26143. https://doi.org/10.1021/acs.jpcc.0c08160
16. Miyoshi H, Miki M, Hirano S, Shimizu A, Kishi R, Fukuda K, Shiomi D, Sato K, Takui T, Hisaki I, Nakano M, Tobe Y (2017) Fluoreno[2,3-b]fluorene vs indeno[2,1-b]fluorene: unusual relationship between the number of π electrons and excitation energy in m-quinodimethane-type singlet diradicaloids. J Org Chem 82(3):1380–1388. https://doi.org/10.1021/acs.joc.6b02500
17. Ito S, Minami T, Nakano M (2012) Diradical character based design for singlet fission of condensed-ring systems with 4nπ electrons. J Phys Chem C 116(37):19729–19736. https://doi.org/10.1021/jp3072684
18. López-Carballeira D, Zubiria M, Casanova D, Ruipérez F (2019) Improvement of the electrochemical and singlet fission properties of anthraquinones by modification of the diradical character. Phys Chem Chem Phys 21:7941–7952. https://doi.org/10.1039/C8CP07358A
19. Omar OH, Padula D, Troisi A (2020) Elucidating the relationship between multiradical character and predicted singlet fission activity. ChemPhotoChem 4(10):5223–5229. https://doi.org/10.1002/cptc.202000098
20. Borislavov L, Nedyalkova M, Tadjer A, Aydemir O, Romanova J (2023) Machine learning-based screening for potential singlet fission chromophores: the challenge of imbalanced data sets. J Phys Chem Lett 14(45):10103–10112. https://doi.org/10.1021/acs.jpclett.3c02365
21. Stanger A (2022) Singlet fission and aromaticity. J Phys Chem A 126(43):8049–8057. https://doi.org/10.1021/acs.jpca.2c04146
22. Baird N (1972) Resonance and aromaticity in the lowest 3π-π* state of cyclic hydrocarbons. J Am Chem Soc 94(14):4941–4948. https://doi.org/10.1021/ja00769a025
23. El Bakouri O, Smith JR, Ottosson H (2020) Strategies for design of potential singlet fission chromophores utilizing a combination of ground-state and excited-state aromaticity rules. J Am Chem Soc 142(12):5602–5617. https://doi.org/10.1021/jacs.9b12435
24. Zeng W, El Bakouri O, Szczepanik DW, Bronstein H, Ottosson H (2021) Excited state character of Cibalackrot-type compounds interpreted in terms of Hückel-aromaticity: a rationale for singlet fission chromophore design. Chem Sci 12:6159–6171. https://doi.org/10.1039/D1SC00382H
25. Fallon KJ, Budden P, Salvadori E, Ganose AM, Savory CN, Eyre L, Dowland S, Ai Q, Goodlett S, Risko C, Scanlon DO, Kay CWM, Rao A, Friend RH, Musser AJ, Bronstein H (2019) Exploiting excited-state aromaticity to design highly stable singlet fission materials. J Am Chem Soc 141(35):13867–13876. https://doi.org/10.1021/jacs.9b06346
26. Messelberger J, Grünwald A, Pinter P, Hansmann MM, Munz D (2018) Carbene derived diradicaloids – building blocks for singlet fission? Chem Sci 9:6107–6117. https://doi.org/10.1039/C8SC01999A
27. Japahuge A, Lee S, Choi CH, Zeng T (2019) Design of singlet fission chromophores with cyclic (alkyl)(amino)carbene building blocks. J Chem Phys 150:234306. https://doi.org/10.1063/1.5099062
28. Ullrich T, Pinter P, Messelberger J, Haines P, Kaur R, Hansmann MM, Munz D, Guldi DM (2020) Singlet fission in carbene-derived diradicaloids. Angew Chem Int Ed Engl 59(20):7906–7914. https://doi.org/10.1002/ange.202001286

29. Jolly PI, Zhou S, Thomson DW, Garnier J, Parkinson JA, Tuttle T, Murphy JA (2012) Imidazole-derived carbenes and their elusive tetraazafulvalene dimers. Chem Sci 3:1675–1679. https://doi.org/10.1039/C2SC20054F
30. Murphy JA (2014) Discovery and development of organic super-electron-donors. J Org Chem 79(9):3731–3746. https://doi.org/10.1021/jo500071u
31. Eymann LYM, Varava P, Shved AM, Curchod BFE, Liu Y, Planes OM, Sienkiewicz A, Scopelliti R, Tirani FF, Severin K (2019) Synthesis of organic super-electron-donors by reaction of nitrous oxide with N-heterocyclic olefins. J Am Chem Soc 141(43):17112–17116. https://doi.org/10.1021/jacs.9b10660
32. de Wergifosse M, Grimme S (2021) Perspective on simplified quantum chemistry methods for excited states and response properties. J Phys Chem A 125:3841–3851. https://doi.org/10.1021/acs.jpca.1c02362
33. de Wergifosse M, Bannwarth C, Grimme S (2019) A simplified spin-flip time-dependent density functional theory approach for the electronic excitation spectra of very large diradicals. J Phys Chem A 123(27):5815–5825. https://doi.org/10.1021/acs.jpca.9b03176
34. de Wergifosse M, Seibert J, Champagne B, Grimme S (2019) Are fully conjugated expanded indenofluorenes analogues and diindeno[n]thiophene derivatives diradicals? A simplified (spin-flip) time-dependent density functional theory [(SF)sTD-DFT] study. J Phys Chem A 123(45):9828–9839. https://doi.org/10.1021/acs.jpca.9b08474
35. Shao Y, Head-Gordon M, Krylov AI (2003) The spin-flip approach within time-dependent density functional theory: theory and applications to diradicals. J Chem Phys 118:4807–4818. https://doi.org/10.1063/1.1545679
36. Wang F, Ziegler T (2004) Time-dependent density functional theory based on a noncollinear formulation of the exchange-correlation potential. J Chem Phys 121:12191–12196. https://doi.org/10.1063/1.1821494
37. Wang F, Ziegler T (2005) The performance of time-dependent density functional theory based on a noncollinear exchange-correlation potential in the calculations of excitation energies. J Chem Phys 122:074109. https://doi.org/10.1063/1.1844299
38. Bernard YA, Shao Y, Krylov AI (2012) General formulation of spin-flip time-dependent density functional theory using non-collinear kernels: theory, implementation, and benchmarks. J Chem Phys 136:204103. https://doi.org/10.1063/1.4714499
39. Casanova D, Krylov AI (2020) Spin-flip methods in quantum chemistry. Phys Chem Chem Phys 22:4326–4342. https://doi.org/10.1039/C9CP06507E
40. Krylov AI (2001) Spin-flip configuration interaction: an electronic structure model that is both variational and size-consistent. Chem Phys Lett 350:522–530. https://doi.org/10.1016/S0009-2614(01)01316-1
41. Krylov AI (2001) Size-consistent wave functions for bond-breaking: the equation-of-motion spin-flip model. Chem Phys Lett 338:375–384. https://doi.org/10.1016/S0009-2614(01)00287-1
42. Krylov AI, Sherrill CD (2002) Perturbative corrections to the equation-of-motion spin-flip self-consistent field model: application to bond-breaking and equilibrium properties of diradicals. J Chem Phys 116:3194–3203. https://doi.org/10.1063/1.1445116
43. Slipchenko LV, Krylov AI (2002) Singlet-triplet gaps in diradicals by the spin-flip approach: a benchmark study. J Chem Phys 117:4694–4708. https://doi.org/10.1063/1.1498819
44. Nishimoto K, Mataga N (1957) Electronic structure and spectra of some nitrogen heterocycles. Z Phys Chem 12:335–338. https://doi.org/10.1524/zpch.1957.12.5_6.335
45. Ohno K (1964) Some remarks on the Pariser-Parr-Pople method. Theor Chim Acta 2:219–227. https://doi.org/10.1007/BF00528281
46. Klopman G (1964) A semiempirical treatment of molecular structures. II. molecular terms and application to diatomic molecules. J Am Chem Soc 86(21):4550–4557. https://doi.org/10.1021/ja01075a008
47. Grimme S (2013) A simplified Tamm-Dancoff density functional approach for the electronic excitation spectra of very large molecules. J Chem Phys 138:244104. https://doi.org/10.1063/1.4811331
48. Bannwarth C, Grimme S (2014) A simplified time-dependent density functional theory approach for electronic ultraviolet and circular dichroism spectra of very large molecules. Comput Theor Chem 1040–1041:45–53. https://doi.org/10.1016/j.comptc.2014.02.023
49. Levchenko SV, Krylov AI (2004) Equation-of-motion spin-flip coupled-cluster model with single and double substitutions: theory and application to cyclobutadiene. J Chem Phys 120:175–185. https://doi.org/10.1063/1.1630018
50. Krylov AI (2008) Equation-of-motion coupled-cluster methods for open-shell and electronically excited species: the hitchhiker's guide to Fock space. Annu Rev Phys Chem 59:433–462. https://doi.org/10.1146/annurev.physchem.59.032607.093602
51. Becke AD (1993) A new mixing of Hartree-Fock and local density-functional theories. J Chem Phys 98:1372–1377. https://doi.org/10.1063/1.464304
52. Dunning TH Jr (1989) Gaussian basis sets for use in correlated molecular calculations. I. The atoms boron through neon and hydrogen. J Chem Phys 90:1007–1023. https://doi.org/10.1063/1.456153
53. std2 (version 2.0.1): a program for computing excited states and response functions via simplified TD-DFT methods (sTDA, sTD-DFT, SF-sTD-DFT, XsTDA, XsTD-DFT, and SF-XsTD-DFT). 2025. https://doi.org/10.5281/zenodo.14849828
54. Epifanovsky E, Gilbert ATB, Feng X, Lee J, Mao Y, Mardirossian N, Pokhilko P, White AF, Coons MP, Dempwolff AL et al (2021) Software for the frontiers of quantum chemistry: an overview of developments in the Q-CHEM 5 package. J Chem Phys 155:084801. https://doi.org/10.1063/5.0055522
55. Jmol: an open-source Java viewer for chemical structures in 3D. http://www.jmol.org/.
56. Stoycheva J, Tadjer A, Garavelli M, Spassova M, Nenov A, Romanova J (2020) Boron-doped polycyclic aromatic hydrocarbons: a molecular set revealing the interplay between topology and singlet fission propensity. J Phys Chem Lett 11(4):1390–1396
57. Sandoval-Salinas ME, Casanova D (2021) The doubly excited state in singlet fission. ChemPhotoChem 5(3):282–293. https://doi.org/10.1002/cptc.202000211
58. Glendening ED, Reed AE, Carpenter JE, Weinhold F NBO Version 3.1.
59. Yamaguchi K (1990). In: Carbo R, Klobukowski M (eds) self-consistent field: theory and applications. Elsevier, Amsterdam, pp 727–828
60. Weinhold F, Landis CR (2012) Discovering chemistry with natural bond orbitals. John Wiley & Sons, Inc., Hoboken, New Jersey
61. Frisch MJ, Trucks GW, Schlegel HB, Scuseria GE, Robb MA, Cheeseman JR, Scalmani G, Barone V, Mennucci B, Petersson GA (2009) Gaussian 09. Gaussian, Inc., Wallingford, CT
62. Xu F, Crespi S, Pacella G, Fu Y, Stuart MCA, Zhang Q, Portale G, Feringa BL (2022) Dynamic control of a multistate chiral supramolecular polymer in water. J Am Chem Soc 144(33):6019–6027. https://doi.org/10.1021/jacs.2c01063
63. Solel E, Kozuch S (2018) Tuning the spin, aromaticity, and quantum tunneling in computationally designed fulvalenes. J Org Chem 83(18):10826–10834. https://doi.org/10.1021/acs.joc.8b01541
64. Oklem G, Song X, Toppare L, Baran D, Gunbas G (2018) A new NIR absorbing DPP-based polymer for thick organic solar cells. J Mater Chem C 6:2957–2961. https://doi.org/10.1039/C8TC00113H

65. Poater A, Ragone F, Giudice S, Costabile C, Dorta R, Nolan SP, Cavallo L (2008) Thermodynamics of N-heterocyclic carbene dimerization: the balance of sterics and electronics. Organometallics 27(12):2679–2681. https://doi.org/10.1021/om8001119
66. Messelberger J, Kumar M, Goodner SJ, Munz D (2021) Wanzlick's equilibrium in tri- and tetraaminoolefins. Org Chem Front 8:6663–6669. https://doi.org/10.1039/D1QO01320C
67. Hahn FE, Wittenbecher L, Boese R, Blaser D (1999) N,N′-bis(2,2-dimethylpropyl) benzimidazolin-2-ylidene: a stable nucleophilic carbene derived from benzimidazole. Chem Eur J 5(6):1931–1935. https://doi.org/10.1002/(SICI)1521-3765(19990604)5:6/3C1931::AID-CHEM1931/3E3.0.CO;2-M
68. Hahn FE, Wittenbecher L, Van DL, Frolich R (2000) Evidence for an equilibrium between an N-heterocyclic carbene and its dimer in solution. Angew Chem Int Ed Engl 39:541–544. https://doi.org/10.1002/(SICI)1521-3773(20000204)39:3/3C541::AID-ANIE541/3E3.0.CO;2-B
69. Aguilar Suarez LE, de Graaf C, Faraji S (2021) Influence of the crystal packing in singlet fission: one step beyond the gas phase approximation. Phys Chem Chem Phys 23:14164–14177. https://doi.org/10.1039/d1cp00298h
70. Felter KM, Grozema FC (2019) Singlet fission in crystalline organic materials: recent insights and future directions. J Phys Chem Lett 10(22):7208–7214. https://doi.org/10.1021/acs.jpclett.9b00754
71. Morrison AF, You ZQ, Herbert JM (2014) Ab initio implementation of the Frenkel-Davydov exciton model: a naturally parallelizable approach to computing collective excitations in crystals and aggregates. J Chem Theory Comput 10(12):5366–5376. https://doi.org/10.1021/ct500765m